Aus dem Walter-Brendel-Zentrum für Experimentelle Medizin,

der Ludwig-Maximilians-Universität München

Direktor: Prof. Dr. med. Ulrich Pohl

The C-terminus of Cx37 as target of nitric oxide dependent modification of gap junction permeability

Dissertation

zum Erwerb des Doktorgrades der Humanbiologie

an der Medizinischen Fakultät

der Ludwig-Maximilians-Universität München

Laurenția-Irina Tănase
aus Călărași, Rumänien
2016

Mit Genehmigung der Medizinischen Fakultät
der Universität München

Berichterstatter:	Prof. Dr. med. Ulrich Pohl
Mitberichterstatter:	Prof. Dr. Christian Kupatt
	Prof. Dr. Christian Schulz
Mitbetreuung durch den promovierten Mitarbeiter:	PD Dr. rer. biol. hum. Petra Kameritsch
Dekan:	Prof. Dr. med. dent. Reinhard Hickel
Tag der mündliche Prüfung:	7.03.2016

Research funded by Marie Curie Initial Training Network- Small Artery Remodeling Network and LMU

To my mother

Dedicata mamei mele

``*Life is not easy for any of us. But what of that? We must have perseverance and above all confidence in ourselves. We must believe that we are gifted for something and that this thing must be attained.* ``

MARIE CURIE

Table of Contents

Index of Tables

Index of Figures

SUMMARY

Background: The wall of small blood vessels consists mainly of endothelial and smooth muscle cells. To enable a uniform response of the vessel to agonists, a coordination and synchronization of the response of individual endothelial and smooth muscle cells is considered necessary. Such coordination may be achieved by intercellular communication via gap junctions (GJs). GJs are the intercellular channels built by transmembranous proteins, called connexins (Cxs). There are several Cxs expressed in vascular cells – Cx37, Cx40 Cx43 and Cx45, of which Cx37 Cx40 and Cx43 are found in the endothelium.

Earlier experiments by our group revealed that the calcium permeability of GJs containing Cx37, is specifically reduced by the endothelial autacoid, nitric oxide (NO) (Kameritsch et al., 2005). Especially the exchange of calcium via myoendothelial junctions, where Cx37 is found to be preferentially located, may be of importance for the endothelial calcium homeostasis, which is essentially involved in endothelial autacoid synthesis and signal transfer (Pogoda, Fuller, Pohl, & Kameritsch, 2014). Therefore, this thesis aimed for a better understanding of the molecular basis by which NO could affect the calcium permeability of Cx37 containing GJ.

Methods: The studies were performed in cultured HeLa cells. The advantages of using HeLa cells are that wild type (wt) HeLa cells do not express Cxs and can be stably transfected to express a defined connexin to establish homotypic GJs. Since native Cx37 is hardly detectably by classic Western blot techniques due to the lack of appropriate antibodies, HeLa cells were transfected with Cx37 to which a green fluorescent protein (GFP) tag was added at the end of the C-terminus of the Cx37 protein (Cx37GFP). In addition to the full length Cx37GFP, mutants were generated lacking increasing parts of the C-terminus: a mutant which lacks the last 14 amino acids (aa) of the C-terminus named HeLadel319; a mutant which lacks the last 37 aa of the C-terminus named HeLadel296; and a full length mutant in which one single tyrosine (Tyr/ Y) at position 332 was exchanged by alanine (A) named HeLaY332A. The cells were characterized using immunofluorescence, polymerase chain reaction, Western Blot and mass spectrometry. The permeability of gap junctions to calcium was tested after loading the cells with the fluorescent calcium indicator (Fura 2-AM). By mechanical stimulation of one single cell with a glass rod, local calcium increases were generated and the spread of the calcium change to adjacent cells was quantified by determining the number of reacting cells in confluent monolayers. All experiments were performed in the presence of suramin to prevent potential paracrine stimulatory effects of adenosine triphosphate (ATP) on cytosolic calcium stimulation by mechanically induced ATP release via hemichannels formed by connexins.

Results: Immunofluorescence imaging using laser scanning confocal microscopy revealed that in HeLaCx37GFP cells, the GFP tags and Cx37 had the same subcellular localization. Furthermore, Cx37 messenger ribonucleic acid (mRNA) and protein were observed in the HeLaCx37GFP cells. Experiments with HeLaCx37GFP cells showed an intact functional coupling as assessed by the spreading of calcium increases to 47±5 % of cells per visual field. Pre-exposure of the cells to NO S-nitroso-N-acetyl-D,L-penicillamine (SNAP), 20 µM (for 20 min) reduced the coupling in a dose dependent manner down to 23±3 %. Similar effects were observed by exposing the cells to acidosis (pH 6.6 for 15 min) and H_2O_2 (100 mM for 15 min). Inhibition of tyrosine phosphatases by orthovandate (100 µM) abolished the inhibitory effect of NO whereas an inhibitor of tyrosine kinases (genistein) exerted similar inhibitory effects as NO did.

Immunofluorescence imaging of the mutant cells HeLadel319 and HeLadel296 revealed no quantifiable differences to Cx37GFP full length cells. The mutant cells were channel competent as revealed by the spread of calcium increases. There was even a tendency towards higher coupling especially in HeLadel319. However, NO treatment had no inhibitory effect anymore on cell coupling though low pH and H_2O_2 still exerted inhibition. In view of the effects of tyrosine phosphatase and kinase inhibition described above, we identified a tyrosine in the last 19 aa of the C-terminus of Cx37 as potential target mediating the NO effects. The full length mutant Cx37 Y332A showed indeed no response to NO anymore though subcellular Cx location was unaltered and the GJ permeability to calcium was even increased. Again, the inhibitory effects of low pH and H_2O_2 were preserved in this mutant.

Further attempts to identify the posttranslational modification of Cx37GFP at tyrosine 332 by mass spectrometry analysis failed. Since, under several cleavage procedures, the last part of the C-terminus of Cx37 could not be recovered with sufficient certainty.

Conclusion: In the present study we showed that Cx37GFP forms functionally intact GJs in HeLa cells which allow the same spread of calcium as wt-Cx37 does. The reducing effect of NO on the spread of the calcium signal via GJ is specific and requires the presence of the last 19 aa in the C-terminus of Cx37 as assessed by the mutants Cx37 del296 and del319. The lack of NO effects after conservative exchange of tyrosine 332 against alanine suggests that a NO mediated modification of this tyrosine forms the molecular basis of the NO mediated inhibition. This may be due to a change of tyrosine phosphorylation since the inhibitor of tyrosine phosphatases, orthovanadate, abolished the NO effect.

ZUSAMMENFASSUNG

Hintergrund: Die Wand kleiner Blutgefäße besteht hauptsächlich aus Endothelzellen und glatten Muskelzellen. Um eine gleichförmige Reaktion des Gefäßes auf Agonisten zu ermöglichen, ist eine Koordination und Synchronisation der Antwort diverser endothelialer und glatter Muskelzellen nötig. Eine solche Koordinierung kann durch interzelluläre Kommunikation über Gap Junctions (GJs) erreicht werden. GJs sind interzelluläre Kanäle welche aus Transmembranproteinen – Connexine (Cxs) genannt - bestehen. In vasukulären Zellen werden Cx37, Cx40m Cx43 und Cx45 exprimiert, von denen Cx37, Cx40 und Cx43 im Endothel zu finden sind.

Frühere Versuche unserer Gruppe zeigten, dass die Calcium-Permeabilität von Cx37 enthaltenden GJs spezifisch durch das endotheliale Autakoid Stickstoffmonoxid (NO) reduziert wird (Kameritsch et al., 2005). Insbesondere der Austausch von Calcium über myoendotheliale Gap Junctions, also Verbindungen zwischen Endothel- und Gefäßmuskelzellen, an denen Cx37 bevorzugt vorkommt, könnte von Bedeutung für die endotheliale Calciumhomöostase sein. Calcium ist ein wichtiges Signalmolekül für die Synthese endothelialer Autakoide (Pogoda, Füller, Pohl, & Kameritsch, 2014). Ziel dieser Arbeit war, zu klären, - welche Strukturen von Cx37 für diese Wirkung von NO auf von Bedeutung sind.

Methoden: Die Untersuchungen wurden in kultivierten HeLa-Zellen durchgeführt. Der Vorteil bei der Verwendung von HeLa-Zellen ist, dass Wildtyp (wt) HeLa-Zellen keine Cxs exprimieren und somit stabil mit definiert mit bestimmten Cxs transfiziert werden können, um homotypische GJs zu etablieren. Da natives Cx37 aufgrund mangelnder Qualität käuflich erhältlicher Antikörper mittels Western Blot schwer nachweisbar ist, wurden HeLa-Zellen mit Cx37 transfiziert, an dessen C-Terminus ein grün fluoreszierendes Protein (GFP) gekoppelt wurde (Cx37GFP). Zusätzlich zum Cx37GFP-Wildtyp Konstrukt wurden Mutanten kloniert, denen verschiedene Abschnitte des C-Terminus fehlten: eine Mutante, der die letzten 14 Aminosäuren (aa) des C-Terminus fehlten (HeLadel319); eine Mutante, der die letzten 37 aa des C-Terminus fehlten (HeLadel296), sowie eine Mutante, die zwar volle Länge besitzt, aber an Position 332 ein Alanin (A) anstatt eines Tyrosins (Tyr/Y) besaß (HeLaY332A). Die Zellen wurden mittels Immunfluoreszenz, Polymerasekettenreaktion, Western Blot und Massenspektrometrie charakterisiert. Die Permeabilität der Gap Junctions gegenüber Calcium wurde durch Beladung der Zellen mit dem fluoreszierenden Calciumindikator (Fura 2-AM) getestet. Durch mechanische Stimulation einer einzigen Zelle mit einer kleiner Pipette wurde eine lokale Calciumerhöhung erzeugt und die Ausbreitung von Calcium auf benachbarte Zellen wurde durch Bestimmung der Anzahl der mit einer Caclium Erhöhung reagierenden Zellen in den Zell-Monolayern quantifiziert. Alle Experimente wurden in Gegenwart von Suramin durchgeführt, um potentielle parakrine stimulatorischen Wirkungen von Adenosintriphosphat (ATP) auf die cytosolische Calcium Konzentration durch mechanisch induzierte Freisetzung von ATP über Connexin-Hemikanäle zu verhindern.

Ergebnisse: Immunfluoreszenz-Bildgebung mittels konfokaler Mikroskopie zeigte, dass in HeLaCx37GFP Zellen eine Co-Lokalisation von GFP und Cx37 vorlag. Außerdem wurden sowohl Cx37 Boten-Ribonukleinsäure (mRNA) als auch Cx37 Protein in den HeLaCx37GFP Zellen beobachtet. Experimente mit HeLaCx37GFP Zellen zeigten eine intakte funktionelle Kopplung, die durch einen Calcium-Anstieg in 47 ± 5% der Zellen pro Gesichtsfeld ermittelt wurde. Eine Inkubation der Zellen mit NO (S-Nitroso-N-Acetyl-D, L-Penicillamin (SNAP), 20 µM für 20 min) reduzierte die Kopplung in einer dosisabhängigen Weise auf 23 ± 3% der Zellen pro Gesichtsfeld. Ähnliche Effekte wurden durch Behandlung der Zellen mit Azidose (pH 6,6 für 15 min) und H2O2 (100 mM für 15 min) beobachtet. Eine Hemmung der Tyrosinphosphatasen durch Orthovandat (100 µM) hob die hemmende Wirkung von NO auf, wohingegen ein Tyrosin-Kinase-Inhibitor (Genistein) eine ähnlich hemmende Wirkung wie NO hatte.

Immunfluoreszenz-Analysen der mutierten Zellen HeLadel319 und HeLadel296 ergab keine messbaren Unterschiede verglichen mit dem „Volle-Länge-Konstrukt“ Cx37GFP. Es gab sogar eine Tendenz hin zu höherer Kopplung vor allem in HeLadel319-Zellen. Eine Behandlung mit NO hatte in diesen Zellen aber keinen hemmenden Effekt mehr auf die Zellkopplung obwohl andere Gap Junction Blocker wie ein niedriger pH-Wert oder H2O2 noch immer eine Hemmung bewirken konnten. Im Hinblick auf die bobachteten Effekte von Tyrosin-Phosphatase- bzw. Tyrosin- Kinase-Hemmung identifizierten wir ein Tyrosin in den letzten 19 Aminosäuren des C-Terminus von Cx37 als potentielles Ziel für die NO-Effekte. Die Mutante Y332A Cx37 zeigte in der Tat keine Reaktion mehr auf NO. Die subzelluläre Cx-Lokalisation der Y332A Cx37 Zellen blieb unverändert und die Durchlässigkeit der GJ für Calcium war sogar erhöht. Die hemmenden Wirkungen von niedrigem pH-Wert und H2O2 blieben auch bei dieser Mutante erhalten.

Weitere Versuche, die posttranslationale Modifikation von Cx37GFP an Tyrosin 332 durch Massenspektrometrie zu ermitteln, schlugen fehl, da nach mehreren Spaltungsverfahren der letzte Teil des C-Terminus von Cx37 nicht mit hinreichender Sicherheit dargestellt werden konnte.

Fazit: In der vorliegenden Studie haben wir gezeigt, dass Cx37GFP funktionell intakte GJs in HeLa-Zellen ausbildet, die die gleiche Ausbreitung von Calcium-Signalen wie in Zellen mit Wildtyp-Cx37 (wt-Cx37) ermöglichen. Die hemmende Wirkung von NO auf die Ausbreitung des Calciumsignals über GJ ist spezifisch und erfordert das Vorhandensein der letzten 19 Aminosäuren des C-Terminus von Cx37, was durch die Mutanten Cx37 del296 und del319 gezeigt werden konnte. Da NO keinen hemmenden Effekt mehr auf Mutanten hatte, die anstatt Tyrosin ein Alanin an Position 332 hatten, liegt der Schluss nahe, dass eine NO-vermittelte Modifikation dieses Tyrosins die molekulare Basis der NO-vermittelten Hemmung bildet. Die Ursache hierfür könnte eine Veränderung der Tyrosinphosphorylierung sein, da der Tyrosin-Phosphatase-Inhibitor Orthovanadat den Effekt von NO aufheben konnte.

I. INTRODUCTION

I.1 Structure and function of blood vessels

Blood vessels have a variety of functions: transport of the blood from and to the heart, transport of oxygen from the lung to peripheral organs, and they allow for the exchange of oxygen, carbon dioxide, water and small molecules between the blood and surrounding tissues in the capillary regions of the circulatory system.

The vascular functions are necessary for individual cells in their synchronized actions. Modifications in the diameter of the vessels and also their blood flow can only be achieved with coordinated diameter change along the vascular bed (A. Harris, 2009). All blood vessels except the capillaries have in principle a 3 layered structure of the vascular wall comprising of an intima, formed by endothelial cells (EC) and their basal lamina. The second layer, the media, is built mainly by smooth muscle cells (VSM). The outermost layer, the adventitia, contains mainly fibroblasts, pericytes and other non-muscle cell types (Majesky, Dong, Hoglund, Mahoney, & Daum, 2011) (Figure I-1). The main vascular cells, the EC as well as the VSM, can communicate with each other since they are coupled by intercellular connections, called gap junctions, GJs (A. Harris, 2009). Previous studies have shown (Kurjiaka & Segal, 1995; de Wit et al., 2000) that EC can communicate via gap junctions over a relatively long-distance, thereby contributing to the coordination of vessel diameter changes. A study of Kameritsch et al. demonstrates that calcium can be transferred via gap junctions to adjacent endothelial cells thereby regulating the endothelial response to vasoactive agonists (Kameritsch, Pogoda, Ritter, Munzing, & Pohl, 2012).

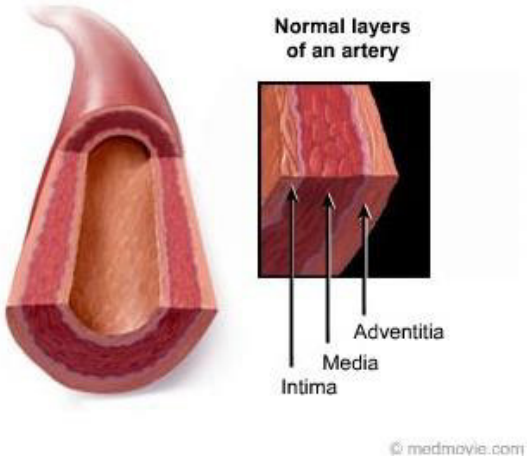

Figure I-1 Vascular wall structure. The vascular wall has several layers: intima, media and adventitia. Intima contains the endothelial cells and internal elastic lamina; media has smooth muscle cells and adventitia contains fibroblasts (http://pixgood.com/artery-wall-anatomy.html).

Regulation of blood flow in arteries comprises several pathways. Vasomotor stimuli can affect the VSM directly, thereby inducing vasoconstriction or – relaxation, or they act indirectly on EC eliciting the release of endothelial autacoids. Direct effects are, for example, a relaxation of VSM due to changed partial pressures of carbon dioxide (pCO_2) or pressure of oxygen (pO_2) induced by metabolic activity of the cells. The sympathetic neurotransmitter, norepinephrine can also produce vasoconstriction when binding to VSM alpha receptors. Especially in skeletal muscle vessels, epinephrine and norepinephrine can also induce vasodilatation by stimulating beta adrenergic receptors under special conditions. Other important hormones regulating the tone of VSM are e.g. natriuretic peptides or angiotensin II, respectively.

EC-dependent vasomotor responses (predominantly vasodilation) are elicited by mechanical (shear stress) or local humoral stimuli such as histamine, bradykinin, or ATP. Endothelium dependent dilatation is mediated by factors like nitric oxide (NO) or the endothelium derived hyperpolarizing factor (EDHF) finally inducing a relaxation in the smooth muscle cells (SMC). Of note, at least in small arterioles which are most important for the control of tissue blood flow, underlying VSM can also be influenced via myoendothelial gap junction communication (Widmaier E. P., 2008; de Wit & Griffith, 2010; Korthuis, 2011; Straub, Zeigler, & Isakson, 2014; Sandow, Senadheera, Bertrand, Murphy, & Tare, 2012).

I.2 Gap Junctions

As pointed out above, the vascular GJs have been implicated in control of vascular tone and blood pressure. These include mainly endothelium-derived hyperpolarization of the underlying smooth muscle (usually termed as EDHF responses) and the conducted vasodilation and constriction in the microcirculatory network (Pogoda et al., 2014; Rummery & Hill, 2004).

Figure I-2 depicts schematically the location of GJs in the blood vessels. They are expressed between cells in the smooth muscle or endothelial layer, but, at least in small arterioles, between SMC and EC (myoendothelial gap junctions MEGJ). The occurrence of MEGJ is inversely correlated with arterial diameter, suggesting that MEGJ play an important role in smaller resistance vessels (Hill, Rummery, Hickey, & Sandow, 2002).

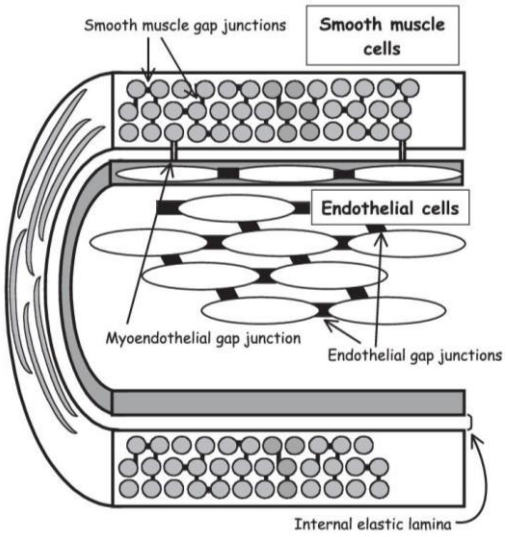

Figure I-2 Localization of cell junctions in vascular wall. Longitudinally orientated endothelial cells are well coupled by large cell junctions, whereas smaller cell junctions are more heterogeneously located among the SMC. In some arteries, the SMC may be coupled to the endothelial cells by small MEGJs that traverse the internal elastic lamina**.** Original picture taken from (Rummery & Hill, 2004).

Figure I-3 shows a thin section of two adjacent cultured fibroblasts. Their cells membranes contain clusters of small intercellular channels. The right part of the picture depicts a freeze fracture image also showing the cluster which consists of GJs (Alberts, 2002; Goodenough & Gilula, 1974), the GJs allow the transfer of molecules from one cell to the other.

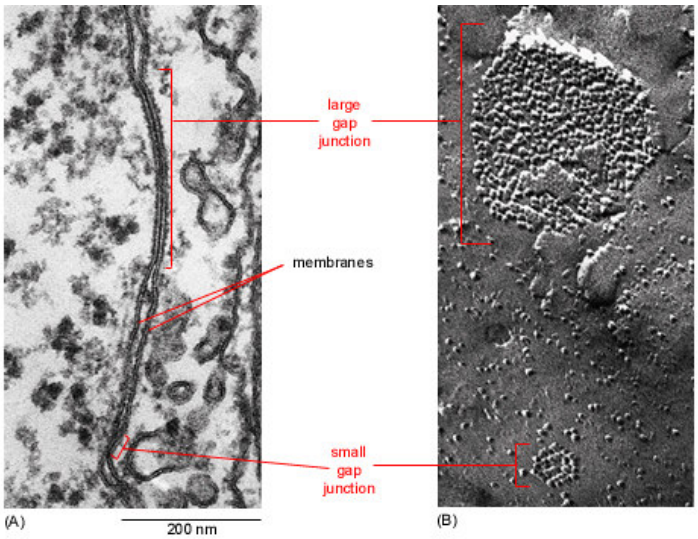

Figure I-3 Gap junctions in fibroblasts (A) depicts a thin-section and (B) a freeze-fracture electronmicrograph where the cluster of homogeneous intramembrane particles are gap junctions. Each intramembrane particle corresponds to a connexon. Original picture taken from (Alberts, 2002).

Gap Junctions are principally formed by a family of transmembrane proteins, the connexins. Connexins are members of a family with 20 proteins in mice and 21 proteins in humans, named after the molecular mass of their complementary deoxyribonucleic acid (cDNA). According to their structure they can also be assigned to an α-group (Cx37, Cx40, Cx43, see Table I-1), β group and γ group (Cx45) (Kumar & Gilula, 1996; Sohl & Willecke, 2003; Johnstone, Isakson, & Locke, 2009). Protein sequence identity mouse versus human is 91% for Cx37, 85 % for Cx40, 98 % for Cx43, 98 % for Cx45 (Sohl & Willecke, 2004).

Human		Mouse	
Protein name	Gene name	Protein name	Gene name
CX43	*GJA1*	Cx43	*Gja1*
CX46	*GJA3*	Cx46	*Gja3*
CX37	*GJA4*	Cx37	*Gja4*
CX40	*GJA5*	Cx40	*Gja5*
--------	--------	Cx33	*Gja6*

Table I-1 The connexin family. The Cx gene names have been adopted from those suggested by Sohl and Willecke and using the phylogenetic tree from Cruciani and Mikalsen. Original table taken from (A. Harris, 2009).

Figure I-4 shows that 6 Cxs (A) form a connexon (B) which are also called a hemichannel. Two connexons located in adjacent cells may couple, thereby forming an intercellular channel which allows passage of small molecules and ions to adjacent cells (C) (Dbouk, Mroue, El-Sabban, & Talhouk, 2009; Goodenough & Paul, 2009). Each GJ has a lumen of about 20 Angstrom (Å) (Berg, 2013).

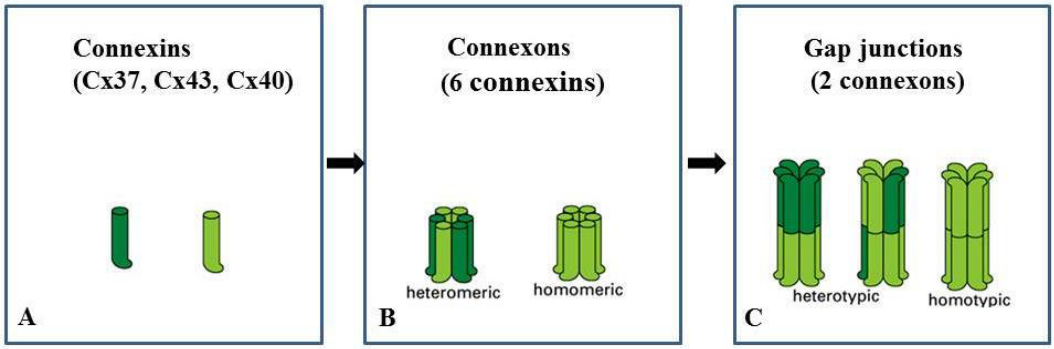

Figure I-4 Schematic representation of gap junctions. GJs are formed from 2 hemichannels (connexons) which may have the same or different composition of Cxs. Connexons have in composition six different or identical Cxs. Picture modified from (Alberts, 2002).

I.2.1 Connexin structure

One Cx has four transmembrane domains (m1, m2, m3, m4), thereby forming two extracellular loops (el1, el2) between m1–m2 and m3-m4. One short cytoplasmic loop (cl) is located between m2-m3. The amino-terminus (NH_2, N-terminus) and carboxyl terminus (COOH, C-terminus) are located intracellularly (Figure I-5). Most of the protein sequence is highly conserved for all types of Cxs. In contrast, the cytoplasmic loop (cl) and especially the C-terminus differ significantly and are responsible for the different functional properties of channels

formed by different Cxs (Morel, Burnier, & Kwak, 2009). The C-terminus acts as a regulatory domain in this context and being a substrate for specific kinases as well as other protein partners (Thomas et al., 2002; Duffy, Delmar, & Spray, 2002; Giepmans, 2004). The regulation of Cx in GJs is specific and this is the reason why Cxs function cannot be replaced by other Cxs (Figueroa & Duling, 2009; Figueroa, Isakson, & Duling, 2004; Haefliger et al., 2006).

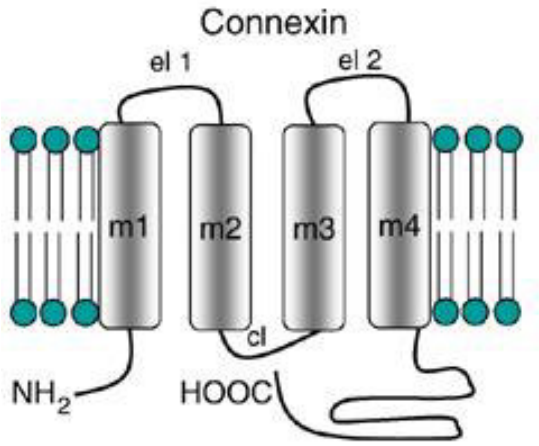

Figure I-5 Connexin structure. Membrane topology of connexins. Diagram of a Cx depicting its orientation according to the plasma membrane (m1 to m4) with the amino-terminal and carboxyl-terminal domain (NH_2 and COOH) located on the cytoplasmic side of the membrane. The protein contains two extracellular loops (el1 and el2) and a cytoplasmic loop (cl). Original picture taken from (Wagner, 2008).

The vascular Cxs (Cx37, Cx40, Cx43 and Cx45) are not expressed uniformly (Berg, 2013). In EC Cx37, Cx40, and Cx43 are found, whereas in SMC Cx43 and Cx45 are mainly expressed (A. Harris, 2009; Rummery & Hill, 2004) but the relative expression differs with regard to vessel type and region (Sandow et al., 2003). In most studies Cx37 and 40 was found in EC only – which agrees with our group findings in the mouse - but Cx37 was also described in VSM, so the vessel`s type might be important (Schmidt, Wolfle, Boettcher, & de Wit, 2008). However; in some vascular regions, expression of Cx37 has also been described in the media (Sandow et al., 2003). The Cx composition of GJs depends on vascular layer and species (Looft-Wilson, Payne, & Segal, 2004; Sandow et al., 2003). At MEGJ, some groups found only Cx37, Cx40, and Cx43 (Haddock et al., 2006; Isakson, Best, & Duling, 2008; Sandow, Neylon, Chen, & Garland, 2006). Therefore each Cxs could play a specific function within the vascular tree and be differently regulated (Schmidt et al., 2008). Simon et al. found that Cx37 is present at the border of EC but not at VSM (Simon & McWhorter, 2003). Isakson et al. located also Cx37 in EC and even more, observed that at the contact point between EC with vascular smooth muscle cells (VSMC) the Cx37 was absent (Isakson & Duling, 2005).

In small resistance arteries, Pogoda et al. demonstrated that within the internal elastic lamina two Cxs endothelial Cx37 and Cx43 are closely located to each other in the whole regions of the internal elastic lamina, where MEGJ can occur. In co-cultured EC and SMC bidirectional

vascular calcium signal propagation at MEGJ is controlled by NO. The inhibition of GJ communication by NO traps the cytosolic calcium within the endothelial cells leading to an intensified endothelial response (Pogoda et al., 2014).

I.3 Connexin 37 / GJA 4

The structure of Cx37 is similar to that of other Cxs, as described above. In brief: 4 transmembrane domains (yellow Figure I-6), 2 extracellular loops (blue), a cytoplasmic loop (cl) with 20 amino acids (aa purple) and cytosolic located N- (black) and C-terminus (red). The C-terminus differs from other Cx (Johnstone et al., 2009). Cx37 has the smallest pore in spite of having the largest unitary conductance > 300 picosiemens (pS) compared to other Cxs (McKinnon et al., 2009; Veenstra, Wang, Beyer, Ramanan, & Brink, 1994; Looft-Wilson et al., 2004).

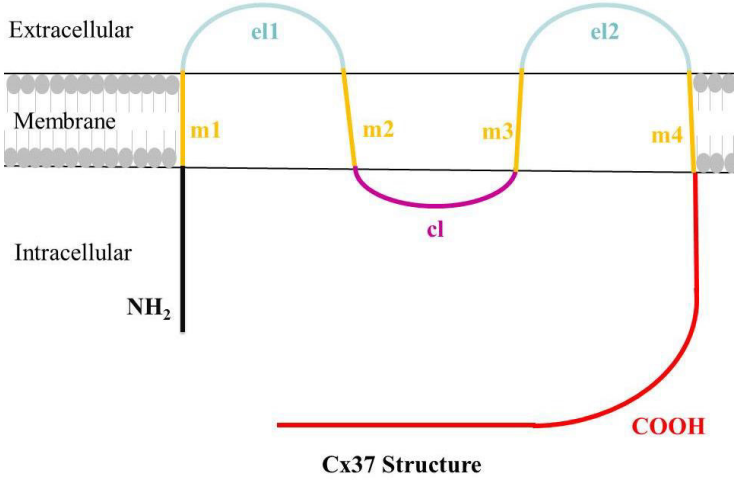

Figure I-6 Schematic representation of Cx37 structure. Cx37 have NH_2 in black, transmembrane domains (m1-4) in yellow, extracellular loops (el1-2) in blue, cytoplasmic loop (cl) in purple and C-terminus (COOH) in red.

As mentioned before, Cx37 is highly expressed in the vasculature and seems to be important for the gap junctional communication of endothelial cells with smooth muscle cells via myoendothelial gap junctions (Pogoda et al., 2014). A decrease of endothelial Cx37, which was found in arteries where endothelial cells overlap atherosclerotic plaques, could therefore be associated with the functional loss of these vessels (Kwak, Mulhaupt, Veillard, Gros, & Mach, 2002; Pfenniger, Chanson, & Kwak, 2013). However, a global knockout (KO) of Cx37 does not lead to any obvious vascular phenotype.

I.3.1 Connexin modifications

Cxs may undergo various posttranslational modifications (PTM) like (de-) phosphorylation, hydroxylation, palmitoylation, nitrosylation, nitration and acetylation (Dbouk et al., 2009). The most studied modifications are phosphorylations of tyrosine (Tyr), threonine (Thr) and serine (Ser). It can be observed in all Cxs being expressed in the vasculature and additionally in Cx31,

Cx32, Cx46, Cx50 and Cx56, while no modification by phosphorylation is known for Cx26 (Dbouk et al., 2009). The C-terminus is the primary target for phosphorylation. Moreover some Cxs are phosphorylated at the cytoplasmic loop (Lampe & Lau, 2004) (Solan & Lampe, 2009a). The majority of phosphorylation occurs at the serine residues but also tyrosine phosphorylation can be observed. A plethora of kinases have been shown to be involved into Cx phosphorylation such as cyclic adenosinmonophosphate (cAMP)-dependent protein kinase (PKA), cyclic guanosine monophosphate (cGMP)-dependent kinase (PKG), protein kinase C (PKC), Ca^{2+}/CaM-dependent kinase II (CaMKII), the Rous sarcoma virus v-Src, cellular proto-oncogene tyrosine-protein kinase Src (c-Src), casein kinases and mitogen-activated protein kinase (MAPK) (Kwak et al., 1995; Lampe & Lau, 2004). Experiments by our group revealed that NO can also affect the permeability of homo- and heterotypic GJs containing Cx37 but the specific mode of the modification is still not known. However it has been shown that it is not cGMP dependent, since the soluble guanylyl cyclase inhibitor - oxadiazole-[4,3-a]-quinoxalin-1-one (ODQ 10 mM, 20 min) had no effect (Kameritsch et al., 2005).

I.4 Nitric oxide

In endothelial cells, NO is produced by the NO synthase (NOS) using L-arginine as a substrate. NO is constitutively produced, but its synthesis is increased when EC are stimulated by shear stress or vasomotor agonists such as histamine, bradykinin or Substance P (see Figure I-7). NO can diffuse to the VSM (Tousoulis, Kampoli, Tentolouris, Papageorgiou, & Stefanadis, 2012), eliciting vasodilation due to an increase of 3`-5`cyclic guanosine monophosphate (cGMP) or activation of potassium channels (Francis, Busch, Corbin, & Sibley, 2010). cGMP activates the protein kinase G (PKG) pathway. The latter involves activation of the myosin light chain phosphatase, activation of calcium-ATPases (and therefore reduction of cytosolic Ca^{2+}) and an inhibition of phospholipase C (PLC)-dependent activation in VSM (Murthy, 2006).

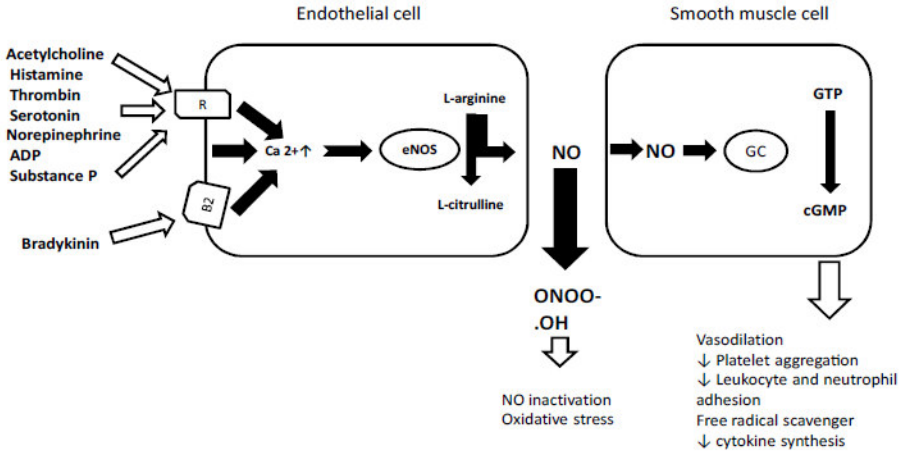

Figure I-7 Synthesis of NO in Endothelial cells. Several agonists (acetylcholine, histamine, thrombin, serotonin) and vasoactive substances (bradykinin) bind to their receptors (R/B2) leading to a calcium increase. The high calcium concentration activates the endothelial NOS (eNOS) which deaminates L-arginine to L-citruline and NO. Original picture taken from (Tousoulis et al., 2012).

NO cannot only be formed in endothelial but also in other cells (e.g. VSM), mainly under inflammatory conditions (Cannon, 1998). It can also be generated pharmacologically by so called NO-donors (Yamamoto & Bing, 2000). They have, independently of the endothelium, the ability to release NO (in vitro and in vivo). They are categorized in different chemical classes (organic nitrates, S-nitrosothiols, sydonimines, sodium nitropusside / SNP and NONOates) (Megson & Webb, 2002). S-nitroso-N-acetylpenicillamine (SNAP), which was used in our study, belongs to the S-nitrosothiols class (Miller & Megson, 2007; Yamamoto & Bing, 2000).

Previous studies of our laboratory showed that NO donors (SNAP and SNP) are able to reduce communication via Cx37 containing gap junctions: NO specifically reduced cGMP-independently of the intercellular communication in the presence of Cx37, which was demonstrated for intercellular dye spreading (Kameritsch, Hoffmann, & Pohl, 2003). In a recent study, Pogoda et al. demonstrated in small resistance arteries that endothelial Cx37 and Cx43 (probably from SMC layer) are located close to each other within the internal elastic lamina and NO controls bidirectional vascular calcium signal propagation at MEGJ in co-cultured EC and SMC (Pogoda et al., 2014). Whilst these previous studies excluded that the NO effects were mediated via cGMP and hence via cGMP-dependent kinase (PKG) dependent phosphorylation at one of the putative PKG phosphorylation sites, (Kameritsch et al., 2005) it remains still elusive how NO is exerting its inhibitory effect on Cx37 containing GJ permeability.

Morel et al. showed two phosphorylation sites at S319 and P319 Cx37 (Morel et al., 2010). Burt et al. suggested equivalent binding sites for Cx37: (compared with Cx43) Ser 275 (for MAPK) and Ser 282 (for PKC) (Burt, Nelson, Simon, & Fang, 2008).

I.5 Hypothesis and aims of the study

We hypothesized that NO may exert its effect by direct or indirect modification of one of the many regulatory sites of the C-terminus of the Cx37. To verify or reject our hypothesis, we therefore aimed to:

1) develop a HeLa cell model expressing GFP tagged Cx37 and to compare its functional properties and subcellular connexin location with the established model of HeLa cells expressing wt Cx37.

2) study the effect of NO on the gap junction dependent transfer of calcium (or a calcium releasing molecule) to adjacent cells and compare it with the gap junction permeability in cells expressing wt-Cx37.

3) identify potential site(s) of NO dependent modulation by studying Cx37 mutants with a deletion of terminal amino acid sequences (Cx37 del 296 and Cx37 del 319) .

4) study the effects of NO of a mutant in which the potential NO target tyrosine is replaced by alanine.

5) identify if possible, the mode of modification by NO of its identified target by mass spectrometry.

We therefore studied the effect of NO on several Cx37 mutants with modified lengths of the C-terminus. These studies were performed in HeLa cells rather than vascular cells, since HeLa cells do not express connexins in their wild type state, so that Cx37 could be expressed in a controlled manner, in contrast to vascular cells which always express several connexins. We focused our studies of GJ function and permeability on the calcium changes in adjacent cells after mechanical stimulation of a single HeLa cell, which induces GJ transfer of calcium or calcium releasing molecules such as inositol 1,4,5-triphosphate (IP_3) via GJs as previously shown by our group (Kameritsch et al., 2012). Since our previous studies also revealed that the commercially available Cx37 antibodies had low quality, we decided to perform all studies in cells in which Cx37 was tagged with GFP.

II. MATERIALS and METHODS

II.1 Materials

II.1.1 Cell lines

Immortal cervix carcinoma cells (HeLa) were used in this work. The cells were a kind gift from Dr. Klaus Willecke (University of Bonn, Germany). HeLa cells, were stably transfected with full length Cx37 or different mutants of Cx37 proteins, all tagged with GFP (Kristin Pogoda).

II.1.2 Plasmides

Cell line	Transfected plasmid
HeLa Cx37	pBEHpac18mCx37
HeLa Cx37GFP	pcDNA4mCx37VLosGFP
HeLa Cx37GFP del319	pcDNA4mCx37 del319GFP
HeLa Cx37GFP del296	pcDNA4mCx37 del296GFP
HeLa Cx37GFP Y332A	pcDNA4mCx37VLosGFP Y332A

II.1.3 Antibodies

Name	Isotype	Dilution	Molecular weight kDa	Application	Company
Primary antibodies					
Cx37	Rabbit anti Cx37 (C-term)	1:1000 5 % milk powder	37	WB, IHC	Invitrogen
GFP	Rabbit polyclonal IgG	1:1000 5 % milk powder	28	WB, IHC	Abcam
GAPDH	Mouse monoclonal IgG1	1:5000 5 % milk powder	36	WB	Chemicon
Secondary Antibody					
Mouse	Goat anti-mouse IgG, HRP conjugate	1:5000 in 5 % milk powder		WB	Calbiochem
Rabbit	Goat anti-rabbit IgG, HRP conjugate	1:5000 in 5 % milk powder		WB	Calbiochem
Rabbit	Alexa Fluor 546 Goat anti rabbit IgG	1:200 in 0.2 % BSA in PBS+		IHC	Invitrogen

II.1.4 Primers

Primer	Sequence	Tm °C	Fragment length basepairs (bp)	Company
For_1Cx37	CCATCTCCCACATCCGATAC	59,4	288	Eurofins MWG GmbH
Rev_1Cx37	CCTCCAGCACACTCTTACAC	59,4		
gfp-for	ATGGCTAGTTCCGGAGGT	55,97	741	Eurofins MWG GmbH
gfp-rev	ACCGTACAGCTCGTCCAT	55,97		
For_1Cx37	CCATCTCCCACATCCGATAC	59,4	1580	Eurofins MWG GmbH
gfp-rev	ACCGTACAGCTCGTCCAT	55,97		

II.1.5 Media and additives

Media	Contains
Freezing medium	10 % DMSO in FCS
HeLa Puromycin medium	10 % NCBS, 100 U/ml penicillin, 100 ug/ml streptomycin, 1 ug/ml puromycin in DMEM
HeLa wt medium	10 % NCBS, 100 U/ml penicillin, 100 ug/ml streptomycin in DMEM
HeLa Zeocin medium	10 % NCBS, 100 U/ml penicillin, 100 ug/ml streptomycin, 200 µg/ml Zeocin, in DMEM

II.1.6 Solutions and buffers

Solution	Contains
4xLaemmli buffer	250 mM Tris-pH 6.8, 8 % SDS, 40 % Glycin, 0.02 % Bromophenol blue, 400 mM β-Mercaptoethanol
Commasie staining solution	0.7 mM Coomassie brilliant blue, 10 % acetic acid, 25 % 2-Propanol
Electrophoresis buffer	124 mM Tris, 960 mM Glycin, 0,5 % SDS
Fura2-AM	4 µmol/L in PBS+
Hepes	144 mM NaCl, 3 mM KCl, 1.2 mM NaH_2PO_4, 3.3 mM $CaCl_2$, 3.2 mM MgCl, 11 mM $C_6H_{12}O_6$, 10 mM Hepes, pH 7.4
Hepes++	30 µM L-NA and 200U/ml SOD in Hepes
PBS-	138 mM NaCl, 6 mM Na_2HPO_4, 1 mM KH_2PO_4, Aqua ad iniectabilia
PBS+	136 mM NaCl, 5 mM KCl, 0.58 mM $MgSO_4$, 0.88 mM $CaCl_2$•$2H_20$, 0.84 mM Na_2HPO_4•$2H_20$, 0.44 mM KH_2PO_4, 5.5 mM $C_6H_{12}O_6$•H_2O, 3.5 mM $NaHC0_3$, Aqua ad iniectabilia 1000 ml
RIPA buffer	10 mM Tris/Cl pH 7.5, 150 mM NaCl, 0.1 % SDS, 1 % TX, 1 % Deoxycholate, 5 mM EDTA
TBS-Tween	50 mM Tris, 150 mM NaCl, 0,1 % Tween 20
Transfer buffer	39 mM Glycin, 48 mM Tris, 0.037 % SDS, 10 % methanol
Trypsin/EDTA	0,25 % Trypsin, 1 mM EDTA-Na_4 in HBSS w/o: Ca, Mg. Phenolrot
TBE buffer	89 mM Tris HCl, 89 mM Boric acid, 2,5 mM EDTA, Aqua ad iniectabilia 1000 ml, pH 8.5
Freezing medium	FCS, 10 % DMSO

II.2 Reagents

Reagent	Company
2-Propanol	Merck KGaA
Acetic acid 100 %	AppliChem GmbH
Acetone	Carl Roth GmbH & Co. KG, Heidelberg, Germany
Agarose	AppliChem GmbH
Antibiotic antimycotic solution (Amphotericin B, Penicillin, Streptomycin)	Sigma-Aldrich Chemie GmbH
Apyrase	Sigma-Aldrich GmbH
Aqua ad iniectabilia	Apotheke Innenstadt, University-Clinic of Munich
Bovine serum albumin	Sigma-Aldrich GmbH
Bromophenol blue	Sigma-Aldrich GmbH
Collagen G	Biochrom AG
Coomassie brilliant blue R-250	Sigma-Aldrich GmbH
Dimethyl sulfoxide	AppliChem GmbH
Disodium ethylenediaminetetraacetic acid	AppliChem GmbH
Disodium hydrogen phosphate dihydrate	AppliChem GmbH
DNA marker (1kb gene)	Thermoscientific
Dulbecco's Modified Eagle Medium	Gibco Invitrogen
Ethanol	Merck KGaA
Ethidium bromide	Sigma Aldrich GmbH
Fetal calf serum	Biochrom
Formaldehyde 37 %	AppliChem GmbH
Fura 2 AM	Calbiochem
Gel Red	Biotium
Glycerol	AppliChem GmbH
Glycine	AppliChem GmbH
Hank's balanced salt solution	Apotheke Innenstadt, University-Clinic of Munich
Hepes	Apotheke Innenstadt, University-Clinic of Munich
Hydrochloric acid	Merck KGaA
Lipofectamine 2000 reagent	Invitrogen
N-nitro-L-arginine	Sigma Aldrich GmbH
Magnesium chloride	Fluka Chemie AG
Methanol	AppliChem GmbH
New born calf serum	NBCS, Biochrom
Nonfat dried milk powder	AppliChem GmbH
PageRulerTM Prestained Protein Ladder	Fermentas
PBS- and PBS+	Apotheke Innenstadt, University-Clinic of Munich
Phenol/Chlororform/Isoamyl alcohol	Carl Roth GmbH & Co. KG
Phenylmethylsulfonyl fluoride	Sigma Aldrich Chemie GmbH
Pluronic	Sigma-Aldrich Chemie GmbH
Potassium dihydrogene orthophosphate	Merck KGaA
Protein kinase inhibitor	Sigma Aldrich GmbH
Restore western blot stripping buffer	Thermoscientific
S-nitroso-N-acetyl-D,L- penicillamine	Biotrend
Superoxide dismutase	Sigma Aldrich GmbH
Sodium chloride	AppliChem GmbH
Sodium dodecylsulfate	AppliChem GmbH

Sodium orthovanadate	Alexis Corporation
Superfect Transfection reagent	Qiagen
Tetramethylethylenediamine	AppliChem GmbH
Tris	AppliChem GmbH
Triton X-100	AppliChem GmbH
Trypsin-EDTA solution	Sigma-Aldrich Chemie GmbH , PAN Biotech GmbH
Tween 20	AppliChem GmbH
Zeocin	Invitrogen 200 µg/ml
β-Mercaptoethanol	AppliChem GmbH
Orthovanadate	Sigma Aldrich Chemie GmbH
Suramin	Sigma Aldrich Chemie GmbH
Genistein	Sigma Aldrich Chemie GmbH

II.2.1 Kits

Name	**Company**
GFP-Trap A nanobeads	ChromoTek
mRNA extraction	Qiagen
S-nitrosylation	Cayman Biochem
RT-PCR Titan one tube	Roche
Chemiluminescence Detection Kit for Horseradish Peroxidase	AppliChem GmbH

II.2.2 Technical equipment

Name	**Company**
Air flow bench	LaminAir HB 2448, Heraeus Instruments
Camera	Imago, Till photonics, Germany
Cell counter	Coulter AcT 8 (Beckman Coulter)
Confocal laser scanning microscope	Leica TCS SP5 (Leica Microsystems)
Cooling centrifuge for falcon tubes	Megafuge 1.0R (Heraeus Instruments)
Cooling centrifuge for microcentrifuge tubes	Biofuge Primo R (Heraeus Instruments)
Electrophoresis chamber	Peqlab Biotechnologie GmbH
Fluorescence microscope	Axiovert 200M (Carl Zeiss) Axiophot (Carl Zeiss) equipped with a AxioCam MRm (Carl Zeiss)
Gel Doc 1000 station	Bio-Rad
Humidified incubator	Sanyo CO_2 Incubator Model MCO-17AI, Sanyo Electric Co. Ltd
Imaging system for western blot analysis (CCD camera)	Digital CCD Camera (ORCA-ER) (Hamamatsu Photonics)
Inverted microscope	Axiovert, Zeiss, Germany
Light microscope	Fluovert FU, Leitz
Micromanipulator	Eppendorf 5171
Monochromator-Polychrom IV	TILL Photonics

pH measurement	PHM 82 Standard pH Meter (Radiometer Copenhagen)
Power Pack P25	Biometra
Power supply Phero-Stab 0310	Biotec-Fischer
Spectrophotometer	Eppendorf
Table centrifuge for microcentrifuge tubes	EBA 12 (Hettich Zentrifugen)
Thermoblock	Eppendorf
Thermocycler for PCR	Mastercycler ep gradient S (Eppendorf AG)
Universal puller	Zeitz Instrumente, Augsburg, Germany

II.2.3 Tools

Name	Company
Glass coverslips 13mm diameter	Helmut Saur
Cell culture dishes 24 well plates and 10 cm dish	BD Biosciences (BD Falcon)
Cryovials	Biozym Scientific GmbH
Polyacrylamide gels 10 % Precise Tris-Glycine Gels	Thermo scientific
Glass pipette GB100F-10 0,58x1.00x100mm	Science products GmbH
Nitrocellulose Blotting Membrane	Peqlab Biotechnologie GmbH
Gel Blotting Papier	Schleicher & Schuell BioScience GmbH
QIAshredder columns	Qiagen

II.3 Methods

II.3.1 Cell culture techniques

II.3.1.1 Cell culture and passaging

HeLa cells were cultivated in a humidified incubator at 37°C and 5 % CO_2. Instruments (glass coverslips and tweezers) were autoclaved before use. All procedures were performed in a laminar air flow hood. A light microscope was used to monitor cell growing.

HeLa wt cells were seeded in Dulbecco's modified Eagle medium (DMEM) supplemented with 10 % new born calf serum (NCBS) and antibiotics (100 U/ml penicillin and 100 µg/ml streptomycin, HeLa wt medium). HeLa Cx37 medium additionally contained puromycin (1 µg/ml). HeLa Cx37GFP cells and all mutants were cultivated in HeLa wt medium supplemented with Zeocin (200 µg/ml). Cells were passaged after reaching confluence and cultivated in different cell culture dishes (60 mm, 100 mm and 24 well plates). To detach cells from the bottom of the culture dish, cells were washed with PBS+ and then incubated in a solution containing 0.5 % trypsin and 0.2 % EDTA. After 5 minutes the detached cells were suspended in the appropriate cell culture medium. The cell suspension was transferred to new cell culture dishes and diluted to the desired concentration with fresh cell culture medium.

II.3.1.2 Transfection of HeLa wild type cells

HeLa cells were stably transfected with full length Cx37 or different mutants of Cx37 proteins, all tagged with GFP (Table II.1.2) (Elfgang et al., 1995).

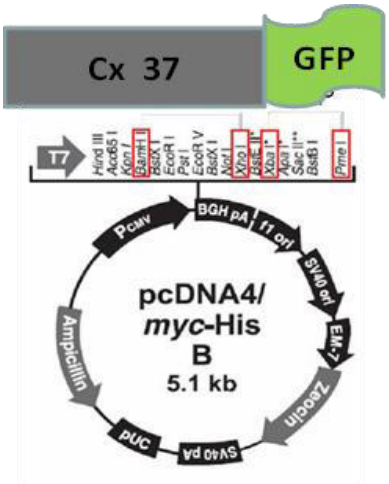

Figure II-1 Map of plasmid pcDNA4 used in transfection. Picture modified from (J. V. Behrens, 2011)

Cells were either transiently or stably transfected. After transient transfections of the cells, deoxyribonucleic acid (DNA) was not integrated into the eukaryotic genome of cell and was lost during mitosis. During stable transfection plasmid DNA was integrated in the cell genome and was transmitted to the descendants. To select the stable transfected cells, the DNA plasmid contained a gene which conferred them antibiotic resistance (Figure II-1).

The transfection was performed using Lipofectamine 2000 reagent. HeLa wt cells were seeded in 6 well or 24 well plates in medium without antibiotics at the appropriate density as to reach a 90-95 % confluence the next day. The transfection was done according to the kit protocol. In short:

1. DNA was diluted in the appropriate amount of medium without serum.
2. Lipofectamine 2000 transfection reagent was diluted in the appropriate amount of Opti-MEM Reduced Serum Medium and incubated for 5 minutes at room temperature (RT).
3. After incubation time, the diluted DNA and Lipofectamine were combined, mixed gently and incubated for 20 minutes at room temperature.
4. The complexes were added to each well containing cells and medium. Cells were cultivated at 37^{o}C in a 5 % CO_2 incubator for 6h. After 6h, medium was changed with wt type medium and cells were grown up for 18-48h.

In the final stage, the medium was removed and selection medium containing Zeocin was added. After this, the cells were used for Western Blot, RT-PCR, and calcium measurements.

HeLa wt cells were transfected with differently modified mouse Cx37 encoding DNA fragments (Figure II-2):

1. HeLa Cx37GFP express Cx37 fused to GFP (Kristin Pogoda).
2. HeLadel319 express GFP-tagged Cx37 which lacks 14 amino acids from its C-terminus (Kristin Pogoda).
3. HeLadel296 express GFP-tagged Cx37 which lacks 37 amino acids from its C-terminus (Kristin Pogoda).
4. HeLaY332A express GFP-tagged Cx37 which carries a mutation at position 332 where a tyrosine (Y) was changed to an alanine (A) (Kristin Pogoda).

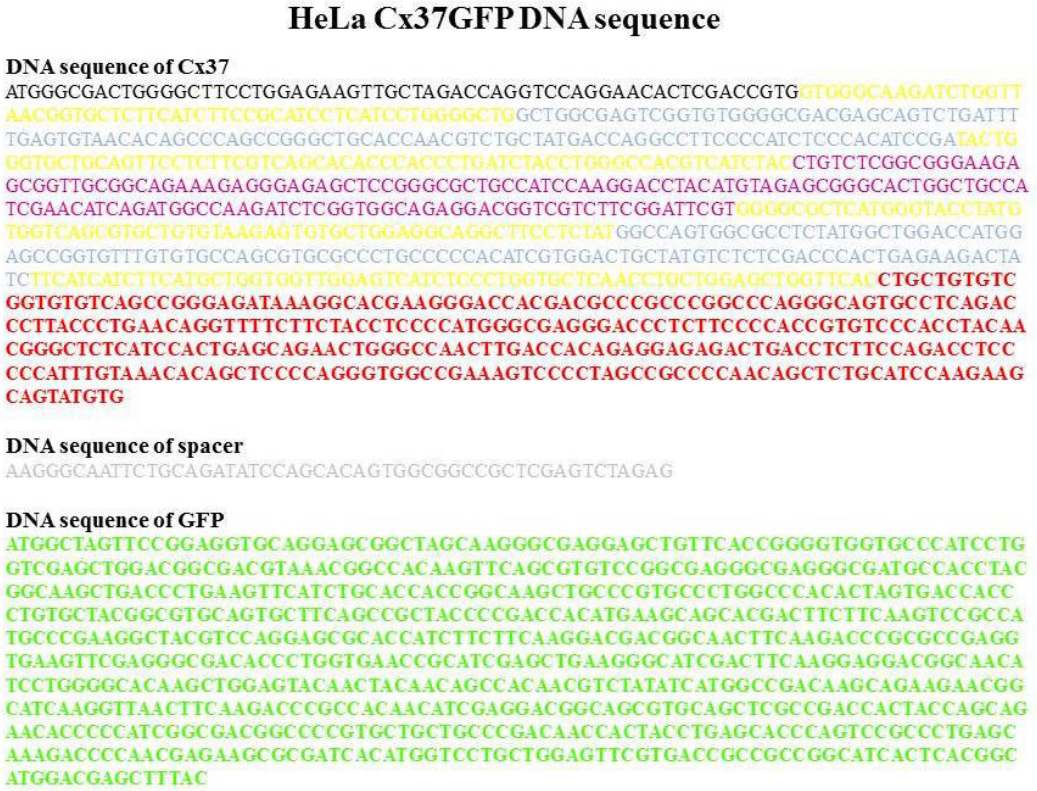

Figure II-2 HeLa Cx37GFP DNA sequence using different colors for each sequence: N-terminus (black), 4 transmembrane domains (yellow), 2 extracellular loops (blue), a cytoplasmic loop (purple), C-terminus (red) and GFP (green). Gray is the DNA spacer.

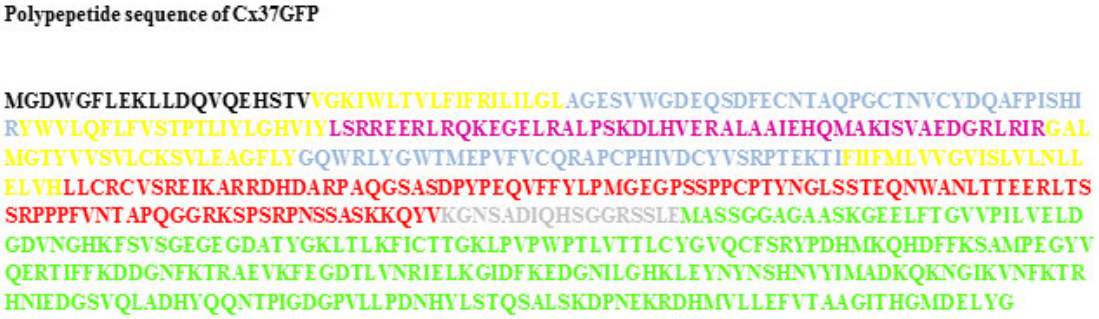

Figure II-3 Polypeptide sequence of Cx37GFP. The same colors were used for the polypeptide sequence as in the previous picture.

Figure II-4 depicts a schematic representation of Cx37GFP and variants using different colors for each domain: N-terminus (black), 4 transmembrane domains (yellow), 2 extracellular loops (blue), a cytoplasmic loop (purple), C-terminus (red) and GFP (green). In variant Y332A the point mutation located at position 332 is marked in red, del319 lacking last 14 aa is marked in dark green and del296 lacking 14 aa is marked in purple. The same colors were used for the DNA and polypeptide sequence.

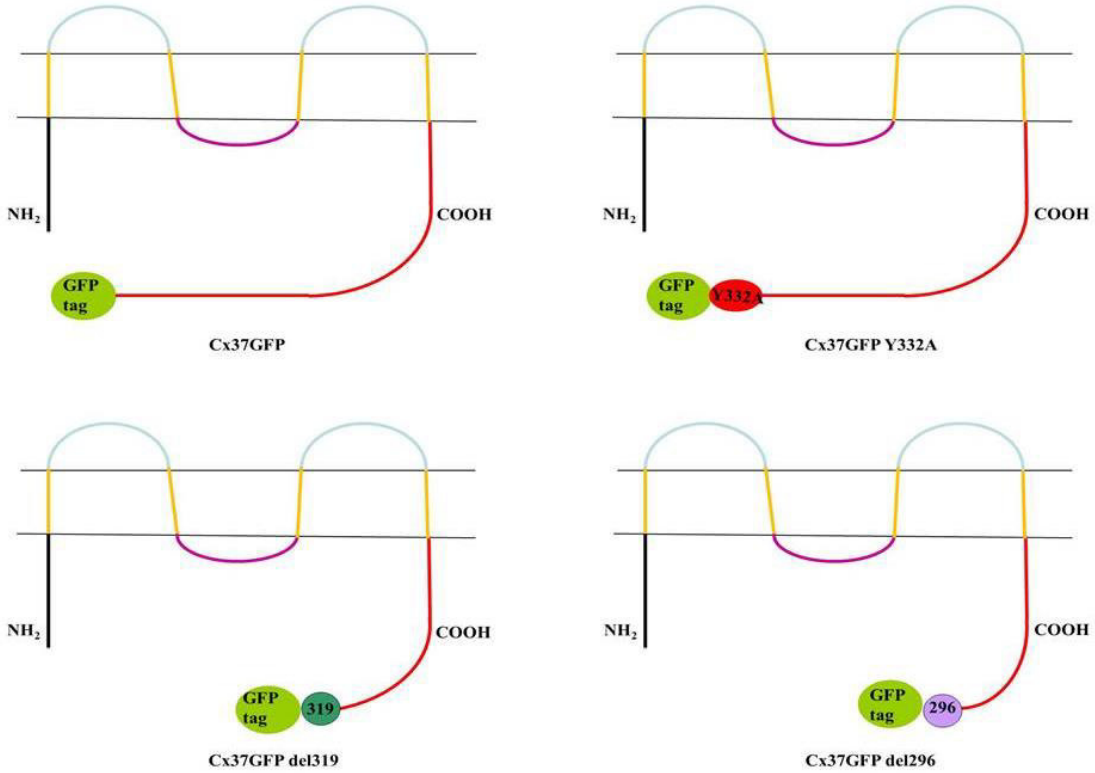

Figure II-4 Schematic representation of Cx37 and Cx37 mutants tagged with GFP at C-terminus

II.3.1.3 Cell freezing and thawing

For freezing, HeLa cells were detached after incubation with trypsin for 2 to 5 minutes, centrifuged (to remove the trypsin) and the cell pellet was suspended in an appropriate amount of freezing medium (FCS and 10 % DMSO). Afterwards, cell solutions were transferred to cryovials, frozen for 24 hours at -80°C and thereafter stored for preservation in liquid nitrogen (-196°C).

For thawing, the cryovials were transferred from liquid nitrogen to 37°C. After 5 minutes, the cell suspension was transferred from the cryovials in a tube with fresh cell culture medium and centrifuged at 1050 rounds per minute (rpm) for 10 min to remove the DMSO. The cell pellet was suspended in specific medium for each type of HeLa cells, plated in culture dishes and placed in the incubator (37°C and 5 % CO_2). After 24 hours, cells were subcultured and used for experiments.

II.3.2 Sample preparation and treatment of cells

One day before experiments cells were seeded onto glass coverslips (13 mm diameter, coated with collagen I (10 µg/ml), and placed in a 24 well plate) or on 10 cm Petri dishes with the specific medium for each type of cells. For each condition the density of the cells allowed them to reach 80 % confluence the next day. At the next day the 24 well plates were rinsed twice with PBS+ and further processed for immunofluorescence assays and calcium measurements. For immunoprecipitation with GFP beads and Western Blot experiments the cells cultured on the 10

cm Petri dishes were washed two times with PBS+ and incubated with different substance as presented in Table II-1. Afterwards, the cells cultured on the 10 cm Petri dishes (see Figure II-5) were detached with trypsin, centrifuged to remove trypsin and the cell pellet was used for further experiments: 1) SDS buffer was added to samples for Western Blots; 2) immunoprecipitation with GFP nanobeads and 3) Protein S-nitrosylation.

Table II-1 Tabel for substances used for treatment of the cells

Substance	Concentration used	Solution	Incubation time
SNAP	2 µM, 0.2 µM, 20 µM	Hepes++	20 min
SNAP + orthovanadate	2 µM SNAP, 100µM orthovanadate	Hepes++	20 min
genistein	100 µM	Hepes++	15 min
orthovanadate	100 µM	Hepes++	15 min
pH 6,6		Hepes++	15 min
H_2O_2	100 µM	PBS+	15 min
suramin	50 µM	Hepes++	20 min

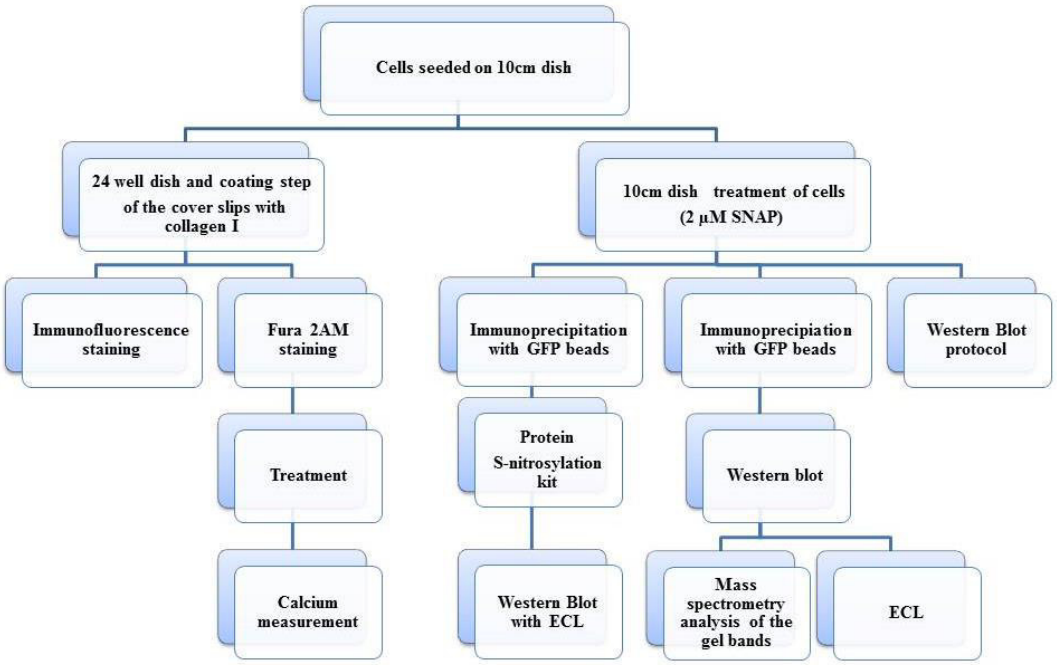

Figure II-5. Schematic representation for sample preparation for experiments

II.3.3 Polymerase Chain Reaction

II.3.3.1 Isolation of total RNA

Total RNA from cells was isolated using the RNeasy Mini Kit according to the manufacturer instructions. $1x10^6$ cells were lysed in RLT buffer (denaturing guanidine-thiocyanate containing buffer with 10 µl/ml ß-mercaptoethanol). QIAshredder columns were used to homogenize the samples (centrifugation 2 minutes at maximum speed). To assure a good binding, ethanol was added before the samples were loaded into the RNeasy Mini spin columns. RNA bound to the column and the contaminants were removed in a centrifugation step of 10,000xg. Total RNA was eluted in an amount of 30 - 50 ul RNase free water and concentration was determined using a spectrophotometer. The samples were stored at -20°C and used for Reverse Transcription-Polymerase Chain Reaction (RT-PCR).

II.3.3.2 Reverse Transcription-Polymerase Chain Reaction (RT-PCR)

A Titan One Tube RT-PCR Kit was used to perform the reverse transcription and PCR in one step (all experiments were done according to the manufacturer`s protocol). This advanced system allows the conversion of RNA messages into amplified DNA fragments. Table II.1.4 contains the primers sequences, which were designed with software primer 3 (Rozen & Skaletsky, 2000).

Primers were diluted in ribonuclease (RNAse) free water (10 pmol/ul) and the ribonucleic acid (RNA) samples were placed on ice. In the meantime the mix containing: water (H_2O), deoxyribonucleotide triphosphates (DNTP), dithiothreitol (DTT), 5xBuffer and RNase inhibitor was prepared. Subsequently, the mix, primers, template and enzyme mix were added in each reaction tub. Single steps and the temperature profile are listed in Table II-2. A Mastercycler was used for thermocycling.

Table II-2 RT-PCR protocol with time, temperature and cycles used for each steps

Time	Temperature	Cycles	Step
30 min	50 °C		reverse transcription
2 min	94 °C		denaturation template
20 sec	94 °C	10	denaturation
30 sec	55 °C	10	annealing
45 sec	68 °C	10	elongation
20 sec	94 °C	35	denaturation
30 sec	55 °C	35	annealing
2 min(+15 sec/cycle)	68 °C	35	elongation
7 min	68 °C		longer elongation

II.3.3.3 Agarose gel electrophoresis

RT-PCR fragments were separated using 1 % agarose gel electrophoresis. Tris-borate-EDTA (TBE) buffer and 1 % agarose were mixed and boiled in a microwave oven 2-3 min until the agarose was dissolved. The solution was cooled to 40 - 50°C and then Gel Red was added.

The 1 % gel was casted in a gel tray and cooled at room temperature to solidify for 1 hour. The samples were diluted with loading buffer (ratio 1:6) and were loaded along with a DNA size marker (1kb gene) in the gel pockets. Electrophoresis was performed at 100 Volts (V) for separation of the fragments. The fluorescence of PCR fragments was observed under UV light with Gel Doc 1000 station (Bio-Rad).

II.3.4 Protein biochemistry

II.3.4.1 Immunoprecipitation with GFP nanobeads

GFP-Trap A nanobeads were used to immunoprecipitate Cx37GFP. Small GFP-binding proteins were coupled to agarose beads (GFP-Trap A), and used to pull down the Cxs tagged with GFP at their C-terminus (Figure II-6).

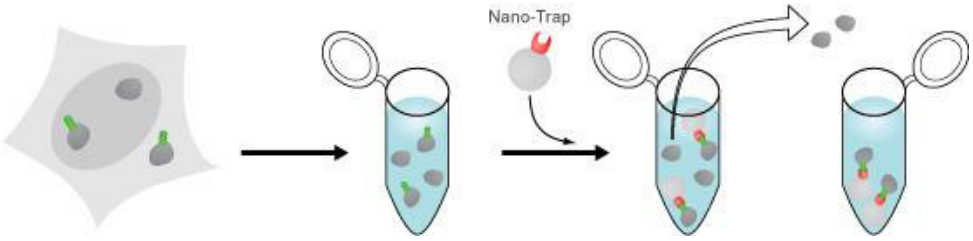

Figure II-6 Schematic representation of Cx37 pull down with GFP Trap A nanobeads (Picture taken from ChromoTek)

Cells were lysed for 30 min in 200 µl RIPA buffer supplemented with inhibitors (1 mM phenylmethylsulfonyl fluoride (PMSF), 1x Protein inhibitor Cocktail) extensively pipetting every 10 min. After centrifugation of the input samples, 50 µl of the supernatant was mixed with 50 µl 4xLaemmli buffer (Laemmli, 1970) and the supernatant was incubated with equilibrated GFP-Trap A beads for 2 hours at 4^{o}C. Cell lysates incubated with the GFP Trap A beads were centrifuged and for non-bound samples, 50 µl of the supernatant were mixed with 50 µl 4xLaemmli buffer. The pellet containing beads bound to GFP-tagged Cx37 was washed with washing buffer to remove the unspecific binding. To elute Cx37GFP from the beads, the pellet was suspended in 100 µl 2xLaemmli buffer and boiled at 95^{0}C for 10 min followed by a centrifugation step. The supernatant containing Cx37GFP (without the beads) and non-bound (eluted) beads were loaded in 10 % acrylamide gel.

II.3.4.2 Western Blot

For detection of specific proteins extracted from cells Western Blots were performed. The procedure relied on: 1) the separation of protein mixtures by size using gel electrophoresis (SDS-Page); 2) the efficient transfer of separated proteins to a solid support (semi-dry blotting); and 3) the detection of target proteins by specific antibodies, visualized as a band on a blotting membrane (detection).

1. SDS-Polyacrylamid gel electrophoresis (SDS-PAGE)

Before loading, the lysed samples were boiled at 95°C for 10 min. The polyacrylamide gels 10 % (range for protein size 15-100 kDa) were placed in the tank with electrophoresis buffer and samples were loaded. A molecular weight marker with colored marker in red at 70 kDa was added to each gel to determine the relative molecular mass of the proteins (Table II-3). The gels ran at 185 V, 60 mA.

Table II-3 The molecular weight of the protein

Protein	Protein size(kDa)
HeLa Cx37	37
HeLaCx37GFP	65
HeLa Cx37GFP del319	63
HeLaCx37GFP del296	60
HeLaCx37GFP Y332A	65

After SDS-Page, the gel was stained with Coomassie brillant blue staining solution and bands were cut from the gel for mass spectrometry analysis or continued with semi-dry blotting to detect the protein bands. The polyacrylamide gels were incubated for 1 hour under agitation in Coomassie brillant blue staining solution and then destained with 10 % acetic acid under agitation; thereafter only the blue protein bands were visible.

2. Semi-dry blotting

Semi-dry blotting was performed to transfer the proteins from the polyacrylamide gel to a nitrocellulose membrane. Membrane and filter paper were soaked in transfer buffer and then placed on the custom-made blotting unit (the gel and membrane were placed between two sheets of blotting paper) and set to 300 V for 80 – 100 min. After semi-dry blotting, the membrane was incubated 1 hour with 5 % nonfat dried milk powder in Tris buffered saline Tween (TBS-Tween /TBS-T) under gentile agitation at room temperature to block non-specific binding.

3. Detection

Incubation with primary antibodies was done (diluted 1:1000 µl in 5 % milk powder in TBS-T) on a shaker at 4°C overnight (Table II.1.3). The first antibodies were removed and the membranes were washed for 5 minutes in TBS-T buffer. Subsequently, the membranes were incubated at room temperature for 1 hour under gentile agitation with secondary antibodies. After 10 minutes washing, the detection of the proteins was done with the Chemiluminescence Detection Kit for Horseradish Peroxidase (luminol-based substrate). To visualize the protein luminescent bands a digital CCD Camera connected to a computer equipped with the Wasabi imaging software was used.

Membrane stripping

The stripping method was used to remove primary and secondary antibodies from the western blot membrane to be able to incubate the membrane with other antibodies. The membrane was incubated with western blot stripping buffer for 15 min at 37°C. After washing with TBS-T, the membrane was blocked 1 h with 5 % milk powder in TBS-T and then incubated with different primary antibodies.

II.3.4.3 Protein S-nitrosylation

After incubation of Cx37GFP cell lysates with GFP beads the samples were used for protein S-nitrosylation detection. The experiments were performed according to the kit protocol. In short: The first incubation step was performed with 500 µl buffer A containing blocking reagent under gentle agitation for 30 minutes at 4°C and then centrifuged for 10 minutes at 4°C at 3.000xg. The second incubation step was done with 4 times the volume of ice-cold acetone for each sample at -20°C for 1 hour. Subsequently, samples were centrifuged at 3.000xg for 10 min at 4°C and then each protein pellet was incubated with 500 µl buffer B containing reducing and labeling reagents for 1 hour at room temperature. Afterwards samples were mixed by inversion with 4 times the volume of ice-cold acetone for each sample followed by incubation at -20°C for 1 hour and centrifugation at 3.000xg for 10 min at 4°C. Samples were suspended in 100 µl washing buffer and then all samples were used for SDS-PAGE. The membrane was blocked with 2 % BSA (to avoid high background signal) for 1 hour followed by incubation with S-Nitrosylation detection reagent for 1 hour under gently agitation at room temperature (Figure II-7).

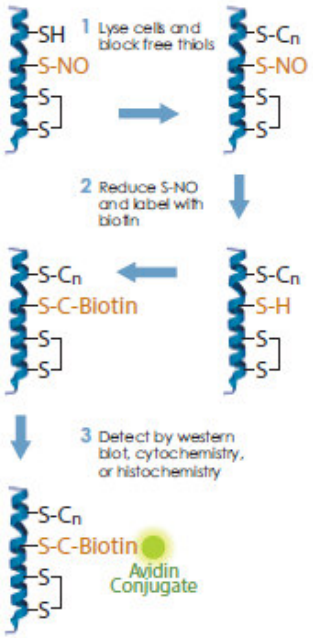

Figure II-7 Diagram of the three-step process of protein nitrosothiol derivitization with biotin (Picture taken from Cayman).

II.3.5 LC-MS/MS (Tandem mass spectrometry) Protein Identification

Experiments were performed in collaboration with Prof. Axel Imhof´s group from the ZfP Munich. Samples were prepared in our laboratory and then sent to their laboratory for mass spectrometry analysis. Mass spectrometry steps were: 1) extraction, fractionation and/or enrichment of protein and/or proteolytically derived peptide mixtures, 2) peptide separation and ionization, 3) measurement and collection of mass spectra and 4) analysis of the obtained data.

After pulldown of Cx37 using anti-GFP agarose beads, proteins were either separated on a SDS-PAGE gel (fractionated) or digested directly from the beads using different sets of proteases (in a first step) (Shevchenko, Tomas, Havlis, Olsen, & Mann, 2006). Proteins were enriched from two biological conditions: control cells and SNAP-treated cells.

II.3.5.1 In gel digestion

Individual protein bands were excised from Comassie briliant blue stained gels and sent for LC-MS/MS analysis. For "in gel" digestion excised protein bands were cut into smaller pieces to facilitate the efficient entering of reagents and enzymes. After several processing steps, the resulting peptide solution was evaporated in a speed vac device. For analysis by LC-MS/MS dried peptide samples were redissolved in 15 µl of 10 % trifluoroacetic acid (TFA) solution. The enzymes used to digest the gel bands were trypsin, chymotrypsin, GluC (Promega, USA) and LysC (Wako Chemicals, Japan)

LC-MS/MS analysis of "in gel" digested samples

Peptide samples were injected into the HPLC system and processed. Peptides eluting from the column were immediately ionized in the ionization source and detected by the LTQ OrbitrapXL hybrid mass spectrometer in the mass range from 300-2000 m/z and analysed for their charge state. Only the 6 most intense signals with charge state 2+ or higher were selected for fragmentation analysis. Peptide fragmentation was carried out using CID activation and generated peptide fragment ions were detected in the ion trap. All raw data were searched against a database containing the human proteome within the MASCOT search algorithm and peptide identification with a MASCOT score of 30 or higher were accepted (Table II-4).

Table II-4 Parameters for MASCOT database search DBMIX

Parameter	MASCOT
Mass error (precursor)	10 ppM
Mass error (fragments)	0.5 Da
Enzyme settings	Trypsin/P (trypsic cleaveage after K or R except they are followed by a P)
Static modification	Carbamidomethylation (C)
Variable/dynamic modifications	Oxidation (M) Phosphorylation (S,T,Y)
Missed cleavages	2

FDR rate estimation	Manual based on score settings No search against reversed database score ≥ 30

II.3.5.2 In solution digestion

The second method of samples digestion was performed directly on the beads (Cx37 bound to GFP beads) without SDS-PAGE separation and included a step for peptide separation on a nanoscale reversed phase (RP) chromatography prior to mass spectrometry analysis (followed by ionisation of the eluting peptides using electrospray ionization, the peptide ions were transferred then directly into the vacuum of the mass spectrometer). For analysis of phosphorylated peptides, a TiO_2-based solid-phase extraction step was introduced. Finally, the samples were injected into the HPLC for LC-MS/MS analysis.

II.3.5.3 LC-MS/MS analysis

The mass and signal intensity of peptides were measured in MS mode of MS instrument and the peptide fragments were detected in MS/MS mode after peptides were fragmented in ions. The raw data were searched within the Sequest and Andromeda search engines against the complete human database (IPI) to test analysis of digests. Phosphopeptides were first identified from a small database containing ~175 entries of human proteins, contaminants and the GFP-tagged Cx37 sequence using Sequest and Maxquant search algorithms. Sequest identified the 4+ and 5+ charge states of the peptide with high confidence in the control and SNAP treated sample. MaxQuant succeeded to identify the 5+ charge state in the SNAP sample. The MASCOT search engine was not able to identify any phosphorylation in Cx37 which might be due to the high charge state of the precursor ion (4+ and 5+). (Table II-5)

Table II-5 Database search settings:

Parameters	**Sequest**	**MaxQuant**
Mass error (precursor)	20 ppM	20 ppM for first search 6 ppm for main search
Mass error (fragments)	0.6 Da	0.6 Da
Enzyme settings	Trypsin or LysC/GluC combination Both fully specific	Trypsin or LysC/GluC combination Both fully specific
Static modification	Carbamidomethylation (C)	Carbamidomethylation (C)
Variable modifications	Oxidation (M) Phosphorylation (STY) Acetylation (Protein N-term)	Oxidation (M) Phosphorylation (STY) Acetylation (Protein N-term)
Missed cleavages	2	3
FDR rate estimation	Manual based on score settings No search against reversed database	Automatic by search against reversed database

Charge / minimal score
2+ / 2.00
3+ / 2.25
4+ / 2.5
5+ / 2.75
6+ / 3.00

- **Cx37GFP identification in HeLa Cx37GFP cells**

MGDWGFLEKLLDQVQEHSTVVGKIWLTVLFIFRILILGLAGESVWGDEQSDFECNTAQPGCTN
VCYDQAFPISHIRYWVLQFLFVSTPTLIYLGHVIYLSRREERLRQKEGELRALPSKDLHVERAL
AAIEHQMAKISVAEDGRLRIRGALMGTYVVSVLCKSVLEAGFLYGQWRLYGWTMEPVFVCQ
RAPCPHIVDCYVSRPTEKTIFIIFMLVVGVISLVLNLLELVHLLCRCVSREIKARRDHDARPA
QGSASDPYPEQVFFYLPMGEGPSSPPCPTYNGLSSTEQNWANLTTEERLTSSRPPPFVNTAP
QGGRKSPSRPNSSASKKQYVKGNSADIQHSGGRSSLEMASSGGAGAASKGEELFTGVVPIL
VELDGDVNGHKFSVSGEGEGDATYGKLTLKFICTTGKLPVPWPTLVTTLCYGVQCFSRYP
DHMKQHDFFKSAMPEGYVQERTIFFKDDGNFKTRAEVKFEGDTLVNRIELKGIDFKEDGN
ILGHKLEYNYNSHNVYIMADKQKNGIKVNFKTRHNIEDGSVQLADHYQQNTPIGDGPVLL
PDNHYLSTQSALSKDPNEKRDHMVLLEFVTAAGITHGMDELYG

Figure II-8 Identified peptides (underlined) in HeLa Cx37GFP cell lysate using Maldi Toff analysis.

II.3.6 Immunofluorescence staining

To visualize the localization of the protein and co-localization with GFP, the immunofluorescence technique was used. Cells were fixed 20 min with 3 % formaldehyde in PBS+, followed by two washing steps with PBS+. Afterwards the cells were permeabilized for 5 min with 0.1 % TritonX-100 in PBS+, then washed twice with PBS+ and incubated with 1 % BSA in PBS+ for 1 h at room temperature to block unspecific protein binding sites. The incubation step of the cells with primary antibodies (Cx37 or GFP Ab) diluted in 0.2 % BSA in PBS+ was performed overnight at 4°C. The next day, the cells were washed at least 3 times followed by 1 h incubation (in the dark) with Alexa Fluor 546-coupled secondary antibodies, diluted 1:200 in 0.2 % BSA in PBS+. For negative control only, the secondary antibody was added to the cells. The coverslips were then transferred to a chamber and a few drops of PBS^+ were added. The localization of Cxs was analysed by using the confocal laser scanning microscope Leica TCS SP 5 equipped with a 63x lens (NA 1.4 oil). Connexins tagged with GFP were analysed at an excitation wave length of 488 nanometer (nm) and 543 nm. The pinhole was set to 1-2 mm. The sample was scanned with a point illumination by a laser and the fluorescence from the focal plane was collected with a photomultiplier tube at the emission maxima of 515 nm and 570 nm respectively.

II.3.7 Calcium measurements

Functional coupling was analysed using the Fura-2 AM staining, the mechanical stimulation method and a calcium measurement system.

II.3.7.1 Staining

To monitor and measure the intracellular Ca^{2+} concentration, a synthetic fluorescent indicator Fura-2 AM was used for staining the HeLa cells. The absorption of Fura-2 shifts depending on the Ca^{2+} concentration which is detectable by alternately exciting the dye at 340nm or 380 nm and observing the emission at 510 nm (Figure II-9). The ratio of fluorescence at 340/380 nm is proportional to the concentration of free intracellular Ca^{2+}.

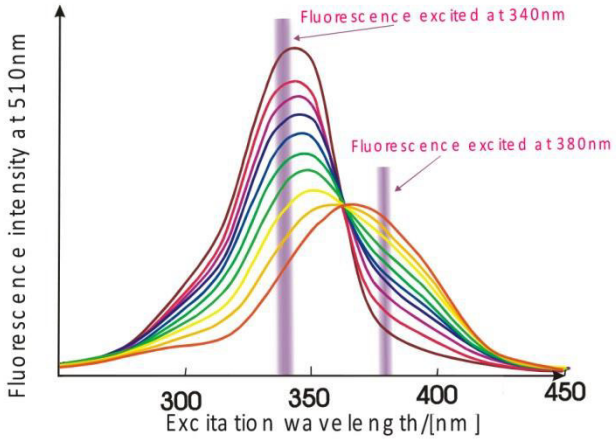

Figure II-9 The 340nm and 380nm wavelengths are highlighted to show typical responses of Fura-2 dye (http://www.wpiinc.com/blog/6)

Fura 2-AM is a membrane permeable dye which is able to prevent hydrophilic carboxyl groups to form esters. Within the cells, the AM groups are cleaved by intracellular esterase enzymes and the dye is trapped inside and is able to bind calcium (Figure II-10) (Hirst, Harrison, Hirota, & Lambert, 1999).

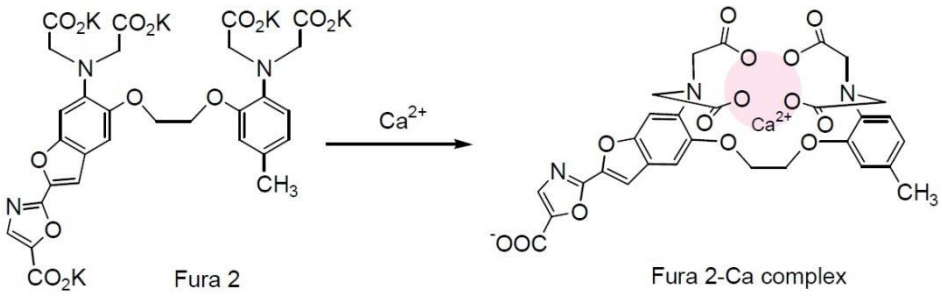

Figure II-10 Fura 2 binding Ca^{2+} after the AM groups were cleaved by esterases

(http://www.dojindo.com/Images/Product%20Photo/F014_fig1.jpg)

The coverslips with the cells were placed into the experimental chamber and were incubated with 4µM Fura 2-AM in Hepes at room temperature, in the dark, for 25 minutes. Cells

were washed with Hepes and then incubated with different substance according to the protocol used (see Table II-1).

II.3.7.2 Mechanical stimulation

After the cells were gently washed with HEPES the experimental chamber was mounted on the microscope table (MGW Lauda RM3), prior heated at 37°C. The temperature of the buffer, in the experimental chamber, was maintained constant during mechanical stimulation. All buffers and solutions were heated up to 37°C.

One single cell was touched with a glass pipette (Zeiss puller diameter of the tip 1 µm) and moved with a micromanipulator (Eppendorf, Hamburg). Mechanical stimulation of one single cell produced an increase in intracellular calcium. The touching experiments were performed in HEPES buffer containing L-NA and SOD and potential ATP signals were blocked with the ATP-degrading enzyme Apyrase (50 U/ml) or the P2 receptor blocker suramin (50 µM) as indicated. In each well 3 touchings were performed in different areas.

The touched cell was named initial cell (cell zero). Neighbouring cells with direct contact to the initial cell were named first ring and cells with direct contact to the cells from the first ring were named second ring (Figure II-11).

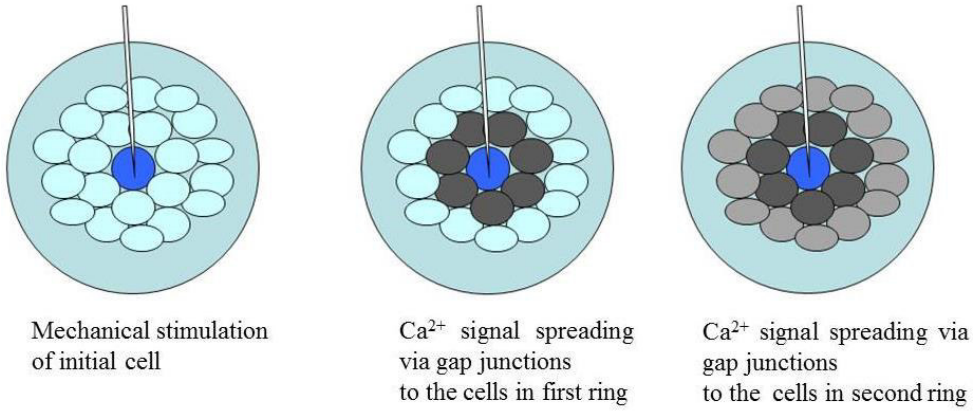

Figure II-11 Schematic representation of mechanical stimulation of cells in first and second ring

II.3.7.3 Calcium measurement

Microscope

Calcium measurements were performed using an inverted microscope (Axiovert, Zeiss, Germany) equipped with a camera (CCD, Imago, Till Photonics, Germany) and a light system (monochromator IV, Till Photonics), both controlled by a computer (TILLvisON, Till Photonics). Experiments were done with a 20x or 40 x lenses.

Excitation/Emission

The stained cells within the visual area were excited at two alternating wavelengths (340 nm and 380 nm) and the fluorescence signal was recorded at 505 nm every 250 ms for 50 s on the computer (movie 340 nm and movie 380 nm).

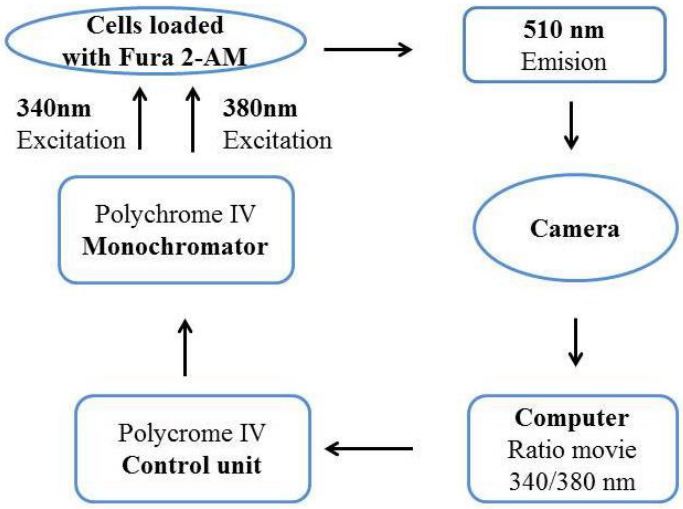

Figure II-12 Microscope system used for Ca^{2+}imaging

After each experiment, the signal was corrected for the background and the signal ratio was calculated by the software as follows: Ratio= (value movie 340nm-background)/ (value movie 380 nm-background). The ratio corresponds with the intracellular calcium signal over time (Bright, Fisher, Rogowska, & Taylor, 1989).

Mean calcium concentration of single cells

In the ratio movie, the program TILLvisON allowed marking the borders of each cell which then were converted in regions of interest (ROI) and the mean intracellular calcium signals of each cell were shown in kinetic graphs (Figure II-13). From this graph, the total number of cells within first and second ring as well as the number of cells showing a calcium increase within the first and second ring was counted. Finally, the percentage of cells that showed an increased calcium level (reacting cells) were calculated. Cells were counted as “reacting” when the calcium level increased by more than 0.025 (ratio, arbitrary units).

Figure II-13 Kinetics graph of several cells after mechanical stimulation

II.3.8 Statistical Analysis

Experiments were performed (n) times in different wells (w) using at least three different cultures (C). Statistical tests were performed using Origin version 8. For normally distributed data we used the t-test to compare two independent samples. In cases where data were not normally distributed we used the Mann – Whitney test instead. In the respective figures legends we indicated the test used. Statistical significance was defined as a *p*- value less than 0.05 indicating an error probability of less than 5 %. Please note, that for reasons of comparability, all values are expressed as means ± standard error of the mean (SEM), although the non-parametric tests do not test for differences of means.

III. RESULTS

III.1 Characterization of full length Cx37 expressed in HeLa Cx37GFP cells

Expression of green fluorescent Cx37:

Initially, cells that express exclusively Cx37 tagged with GFP at its C-terminus were created. HeLa cells were used as they do not express Cxs in the wild type form. The plasmids (Cx37GFP and several GFP tagged mutants) were transfected into HeLa cells and stably transfected cells were exhibiting a green fluorescence as indicated in Figure III-1. The left panel of Figure III-1 depicts a transmission and the right panel the corresponding fluorescence image of the HeLa Cx37GFP cells. In all analysed images, we observed about 90 % fluorescent cells.

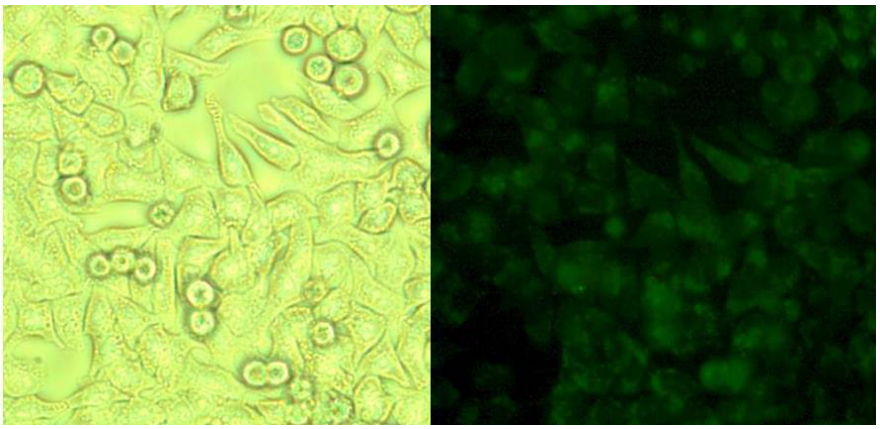

Figure III-1 Fluorescent HeLa Cx37GFP cells tagged with GFP at C-terminus HeLa Cx37GFP cells observed with a fluorescence microscope. The left panel represents the transmission image and the right panel represents the fluorescent image of the cells.

III.1.1 Immunofluorescence staining of Cx37GFP in HeLa Cx37GFP cells

Additionally, the expression of Cx37GFP in the cells was validated by staining the cells with specific antibodies against Cx37 and then analyzing them using a confocal microscope. Figure III-2, depicts two cells (cell 1 and cell 2) showing the green fluorescence of GFP (left panel) and the red fluorescence due to specific Cx37 staining (middle panel) and for each one the nucleus (N) is distinct, as is not stained. The overlay of the two first panels is presented in the right panel and revealed the same localization of the Cx37 and the GFP in the HeLa Cx37GFP cells. Cx37 is mostly distributed within the membrane.

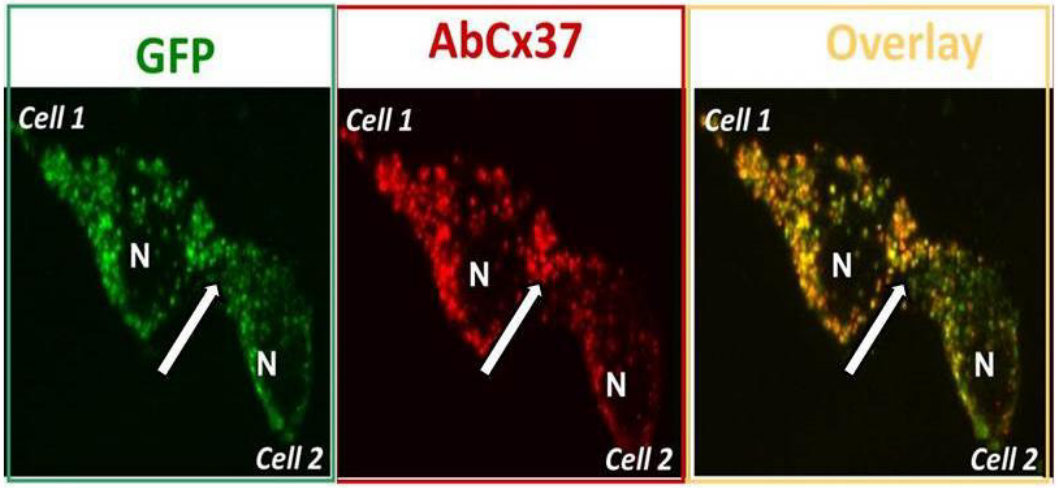

Figure III-2 GFP fluorescence and Cx37 staining showed the same location of Cx37 and GFP in membrane of the cells and also in the cytosol. The left panel represents the autofluorescence of GFP, the middle panel the staining with Cx37 Ab and the right panel the overlay of left and middle panels. The white arrows indicate the contact point between the cells.

III.1.2 Western blot analysis of Cx37GFP

Next, Cx37GFP expression was investigated using SDS-Polyacrylamid gel electrophoresis followed by Western Blot analysis. In HeLa cells expressing Cx37, the protein band was observed at 37 kDa (Figure III-3). Although Cx37GFP protein molecular mass should be 65 kDa (Cx37: 37kD and GFP: 28kDa), a lower double band was observed at 55kDa for HeLa Cx37GFP cells (Figure III-3). The experiments were performed several times with different protocols and protein kinase inhibitors were used to stop the protein degradation. In all experiments we found the 55kDa bands.

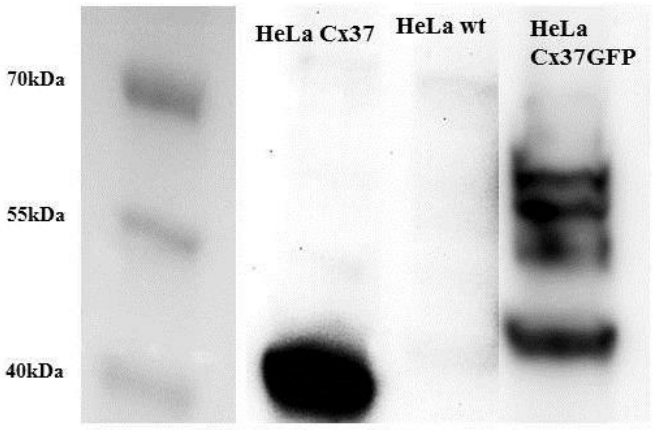

Figure III-3 Cx37 protein expression in HeLa Cx37 (H37) and Cx37GFP (H37GFP) cells with Ab Cx37. The Western Blot showed for control cells HeLa Cx37 a protein band at 37kDa and for HeLa Cx37GFP a band at 55kDa. The antibody used was Cx37.

III.1.3 mRNA expression of Cx37GFP

For analysis of the mRNA expression of Cx37GFP RT-PCR experiments were performed using specific primers for Cx37 and GFP. Primers were designed as following: one set of two primers for a fragment of Cx37 (forward primer starting at base 212 and ending at 231; reverse (rev) primer starting at 499 and stopping at 480) and another set of two for the whole GFP (forward primer starting at 1051 and ending at 1068; reverse primer starting at 1791 and ending at 1774) and Cx37 forward and GFP reverse primers were used for Cx37GFP fragment. To evaluate the length of the RNA molecule we used base pairs (bp) which are pairs of nucleotides joined with a hydrogen bound found in RNA. HeLa Cx37 cells served as positive control for the Cx37 band (see black arrow size 288bp) and HeLa Cx43GFP as positive control for the GFP band (see black arrow size 741bp). As negative controls HeLa Cx37 (with primer for GFP fragment and Cx37 forward primer and GFP reverse primer, see orange arrows), HeLa Cx43GFP with primer for Cx37 fragment (see green arrow) and HeLa Cx37GFP (with Cx43 primer and Cx43 forward primer and GFP reverse primer, see blue arrows) were used. In negative controls, no RT-PCR bands could be observed. In HeLa Cx37GFP cells three RT-PCR products were observed one at 288bp for Cx37 (indicated with a black arrow) and second product at 741bp for GFP (indicated with a black arrow), which corresponded with the size of RT-PCR products from control cells HeLa Cx37 and HeLa Cx43GFP (indicated with a black arrow). The 1580bp (black arrow) was obtained with Cx37 forward primer (For_1Cx37) and GFP reverse (gfp-rev) (see Figure III-4).

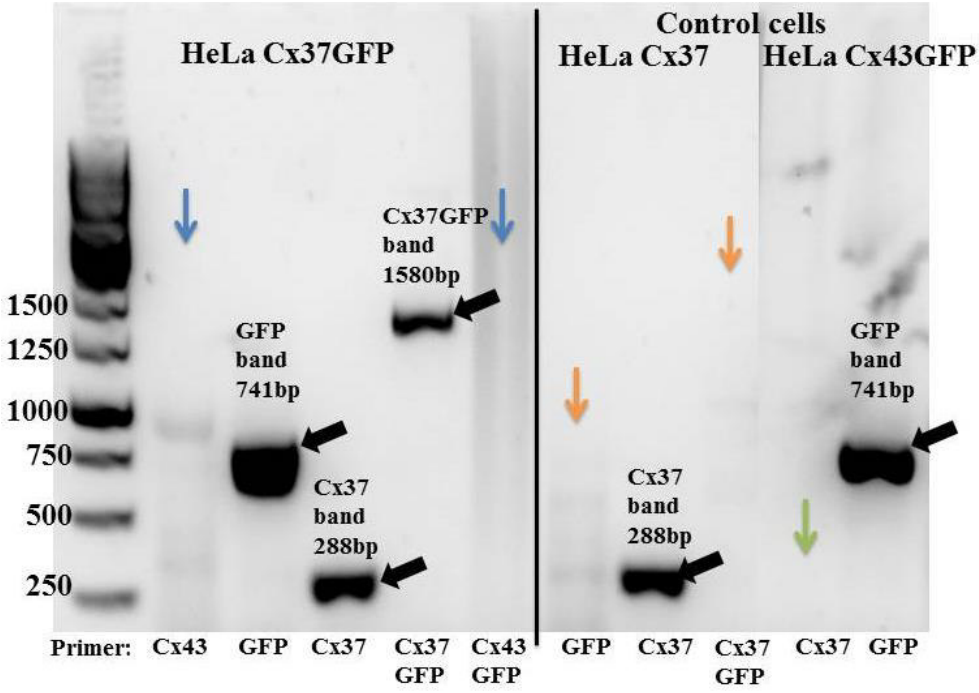

Figure III-4 RT-PCR products in HeLa Cx37GFP, HeLaCx37 and HeLa Cx43GFP cells. Control cells used are HeLa Cx37 and HeLa Cx43GFP. Primer for Cx37 showed in HeLa Cx37GFP and HeLa Cx37 cells a 288bp band and primer for GFP a band at 741bp for HeLa Cx37GFP and Cx43GFP cells. The band at 1580bp was observed in HeLa Cx37GFP cells when primer for Cx37 and GFP primer were used.

III.1.4 HeLa Cx37GFP coupling

To further investigate the permeability of the GJs built by Cx37GFP, calcium measurements in HeLa Cx37GFP cells were performed. Figure III-5 indicates the schematic representation of HeLa Cx37GFP cell coupling defined as the transfer of a calcium signal via gap junctions from the initially stimulated cell to the neighbouring cells. Cells were mechanically stimulated to show that HeLa expressing Cx37GFP were functionally coupled.

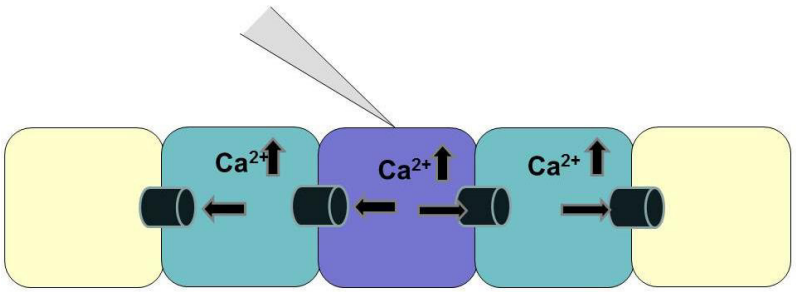

Figure III-5 Schematic representation of mechanical stimulation of HeLa Cx37GFP cells. Mechanical stimulation of one cell led to an increased concentration of calcium. The calcium signal spread via GJ to the neighbouring cells.

Coupling of HeLa Cx37GFP can be observed in Figure III-6. The calcium concentration (ratio 340nm /380nm) of cells before stimulation (A) is shown in blue indicating low concentration of intracellular calcium. Mechanical stimulation (B) led to an increase of calcium concentration in the stimulated cell. With a short time delay (2 sec), the calcium signal propagated via gap junctions to neighbouring cells leading to a calcium increase in these cells (C/D).

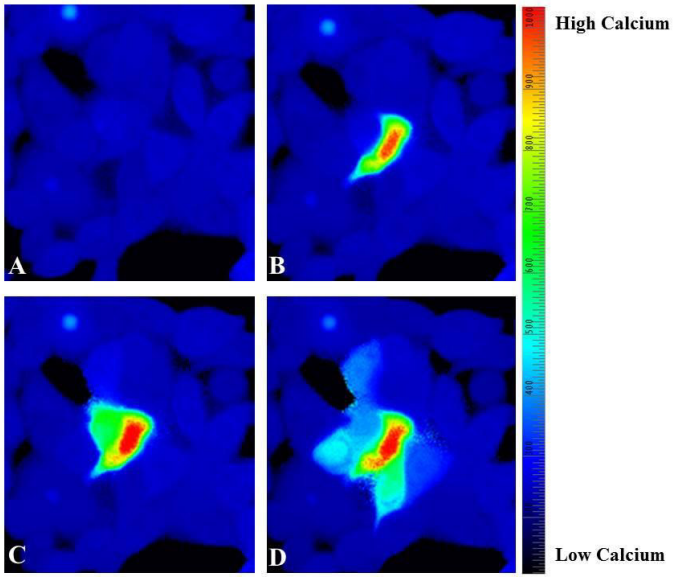

Figure III-6 Coupling of HeLa Cx37GFP cells using mechanical stimulation. Panel A representative ratio of the cells after staining with Fura 2 AM before mechanical stimulation (blue low calcium), the **panel** B indicates the initial cell stimulated with increased calcium concentration, the **panel C** and **D** show the spreading of the calcium signal via GJ to the neighbouring cells.

III.1.5 The effect of different concentrations of SNAP on HeLa cells

The relationship between the SNAP concentration and the cell response was analysed and the dose response curve is shown for different concentrations of SNAP: 0 µM, 0,2 µM, 2 µM, 20 µM, 200 µM (Figure III-7). The potential effect of ATP released due to mechanical stimulation was blocked by inhibition of the P2X receptors (50 µM suramin). Under control conditions (0 µM SNAP) HeLaCx37GFP exhibit a GJ coupling of 50±4 % (n=29, w=18, C=4). SNAP treatment reduced GJ coupling (see Figure III-7) as follows: treatment with 0,2 µM SNAP reduced the coupling to 46±5 % (n=17, w=14, C=5), 2 µM SNAP to 30±8 % (n=12,w=10, C=5), 20 µM SNAP to 17±5 % (n=12, w=12, C=4) and 200 µM SNAP to 16±4 % (n=16, w=7, C=3). Incubation of HeLa Cx37GFP cells with various concentrations of SNAP revealed that 2µM SNAP reduced GJ coupling by 40 % and in all following experiments we used this concentration of SNAP.

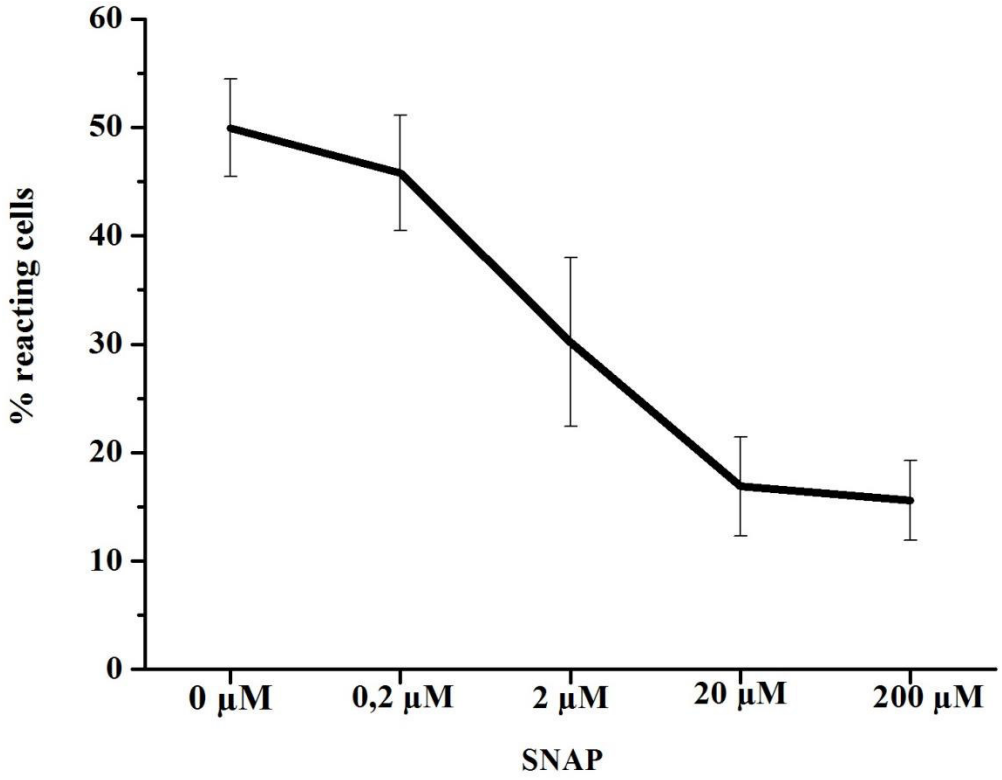

Figure III-7 The concentration dependent effect of 0,2 µM, 2 µM, 20 µM, 200 µM SNAP in HeLa Cx37GFP cells. All experiments were performed using 50 µM suramin and different concentrations of SNAP (0µM SNAP, 0,2 µM SNAP, 2 µM SNAP, 20 µM SNAP and 200 µM SNAP). GJ coupling was reduced by NO treatment compared with GJ coupling in control.

III.1.6 The effect of SNAP, pH 6.6 and H_2O_2 on -Cx37GFP coupling

HeLa Cx37GFP cells were treated with 2 µM SNAP, a Hepes solution of pH 6,6 and 100mM H_2O_2. Figure III-8 A shows that treatment with 2 µM SNAP reduced the number of neighbouring cells showing an increased calcium signal upon mechanical stimulation from 47±5 % (n=25, w=11, C=4 (control) to 23±3 % (n=25, w=11, C=4). At a pH of 7.4 (control) 57±6 %

(n=9, w=5, C=4) of the cells reacted after stimulation whereas at a pH of 6.6 the coupling was reduced to 30±5 % (n=6, w=3, C=2) (Figure III-8 B). Figure III-8 C depicts that coupling of the cells is reduced from 68±8 % (n=11, w=5, C=3) to 23±7 % (n=22, w=10, C=4) after treatment with 100 mM H_2O_2.

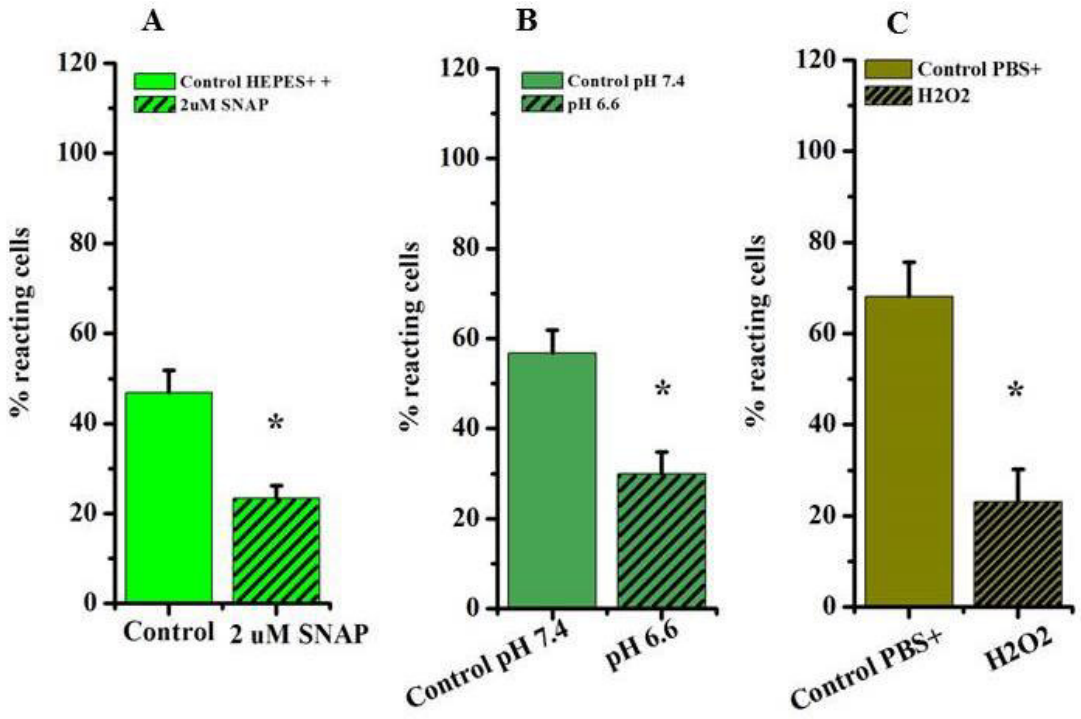

Figure III-8 Functionality of HeLa Cx37GFP cells under control and treatment conditions. A. SNAP reduced the number of reacting cells to 24±3 % (n=25, w=11,C=4) compared to control 47±5 % (n=25, w=11, C=4, t-test); B. For pH 7.4 the GJ coupling is at 57±6 % (n=9, w=5, C=4) whereas for pH 6.6 is reduced to 30±5 % (n=6, w=3, C=2, t-test); C. Treatment with 100mM H_2O_2 decreased the GJ coupling to 23±7 % (n=22, w=10, C=4) versus control 68±8 % (n=11, w=5, C=3, Mann – Whitney test)

III.1.7 The effect of genistein and orthovanadate on Cx37 coupling

To analyse whether tyrosine phosphatases and tyrosine kinases could be involved in post-translational modifications pathways experiments were performed with 100 µM orthovanadate (OV, tyrosine phosphatases inhibitor) and 100 µM genistein (tyrosine kinase inhibitor) to study their effects on intercellular communication. Treatment with 100 µM orthovanadate did not affect GJ coupling (con: 81±3 %, n=24, w=9, C=4; OV 87±3 %, n=23, w=8, C=4 Figure III-9 A). However, after preincubation of the cells with orthovanadate NO had no further effect on intercellular calcium signaling (100 µM orthovanadate and 2µM SNAP: 84±3 %; n=19, w=6, C=3). Figure III-9 B shows experiments with genistein treated cells. Genistein reduced the GJ coupling to 61±5 % (n=27, w=9, C=3) versus control 81±4 % (n=25, w=10, C=3). As OV inhibits all tyrosine phosphatases and genistein all tyrosine kinases which are acting on several tyrosine residues within the connexin, these effects could be the summation of several single effects.

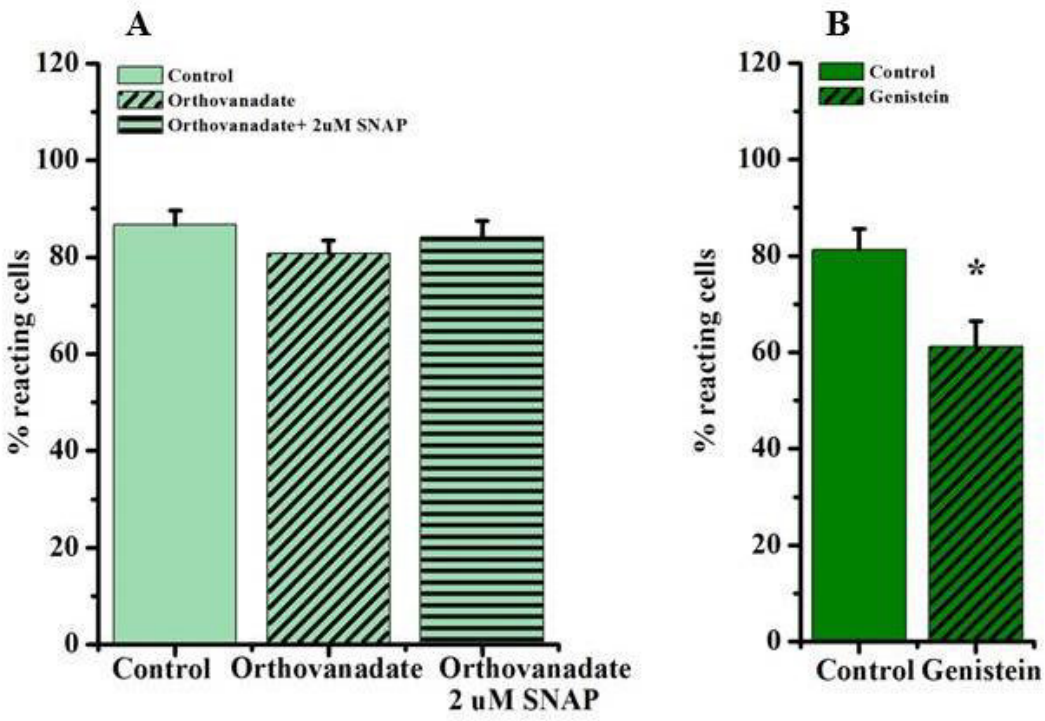

Figure III-9. Effect of genistein and orthovanadate on GJ coupling in HeLa Cx37GFP cells. A despicts the effect of orthovanadate on GJ coupling versus control conditions (n=23, w=8, C=4, one way ANOVA – on ranks). After treatment with orthovanadate SNAP had no further effect on intercellular calcium signaling. B genistein treatment reduced the GJ coupling (Mann – Whitney test).

III.1.8 Analysis of posttranslational modifications of Cx37GFP induced by NO

Several posttranslational modifications of Cx37 (e.g. phosphorylation, nitration) could be induced by NO. To identify the possible post-translational modification and the site of the modifications we used Western Blot, S-nitrosylation and mass spectrometry analysis.

III.1.8.1 Identification of S-nitrosylated Cx37GFP protein

To reveal other posttranslational modifications like S-nitrosylations, a S-nitrosylation assay was performed with control- and NO- (2 µM SNAP) samples. Western blot experiments revealed several identical bands of S-nitrosylated Cx37 in control and SNAP HeLa Cx37GFP cell lysates samples, consequently samples were prepared with two different protocols, as described below:

1. GFP beads pull down of Cx37GFP followed by S nitrosylation assay and
2. The S nitrosylation method followed by the pull down of the Cx37 with GFP nanobeads.

Both protocols showed bands at the same size for SNAP samples whereas in control samples no bands were observed.

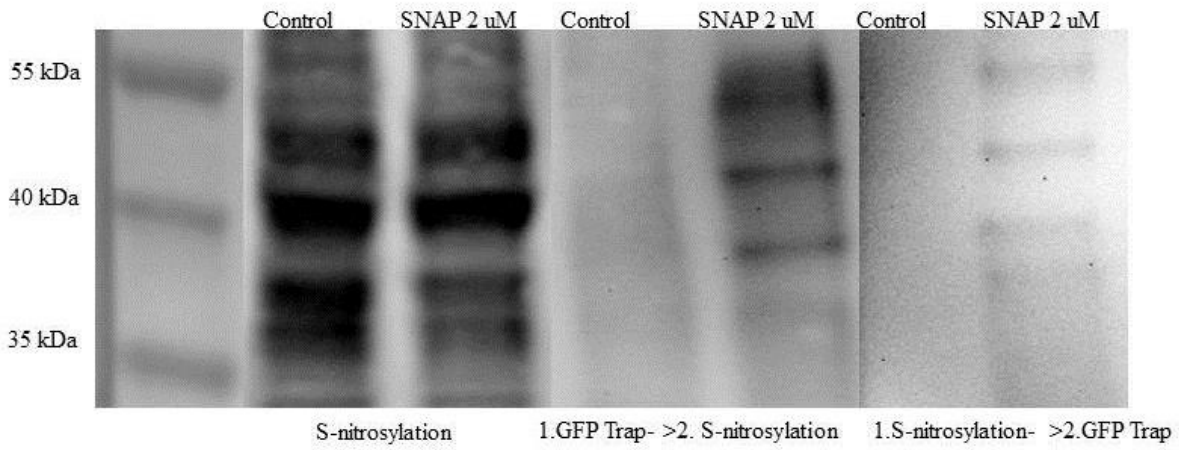

Figure III-10 S-nitrosylation assay in HeLa Cx37GFP cells in control and treatment conditions

III.1.8.2 Mass spectrometry

Posttranslational modifications can be analysed by mass spectrometry. Initially, the protein was identified in HeLa Cx37GFP cells and afterwards the specific modifications induced by NO were analysed.

To identify the Cx37 protein in HeLa Cx37GFP cells, GFP nanobeads pull down was performed and the samples were analysed with mass spectrometry. Figure III-11 depicts the schematically drawing of the transmembrane protein Cx37 with: with the corresponding peptide sequences in the right panel. The Mass spectrometry analysis identified three peptides in the Cx37 samples: one in the extracellular loop - APCPHIVDCYVSRPTEK (see blue arrow) - one in C-terminus - LTSSRPPPFVNTAPQGGRK (see red arrow) - and one in GFP tag - EDGNILGHKLEYNYNSHNVYIMADK (see green arrow). Mass spectrometry analysis revealed the presence of the Cx37 in HeLa Cx37GFP cells.

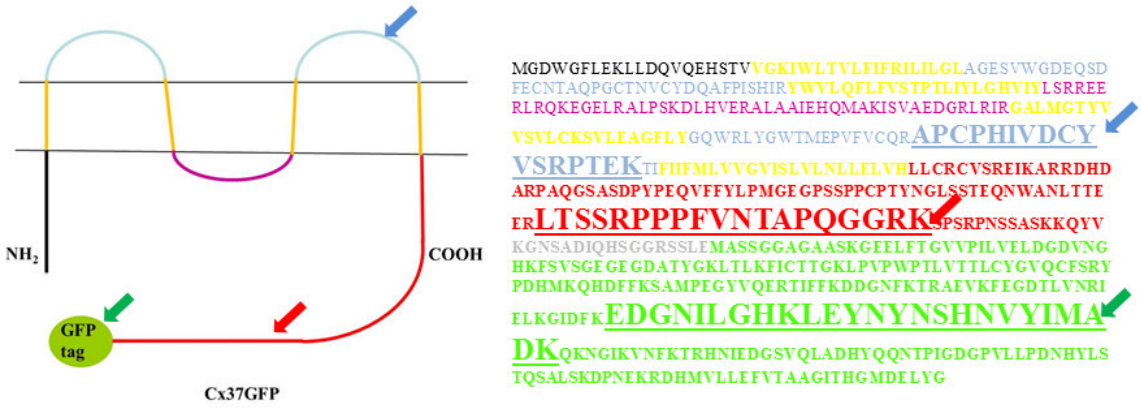

Figure III-11. Identified peptide in HeLa Cx37GFP cell lysate using Maldi Toff analysis

Further mass spectrometry analysis was performed with control- and NO- samples to localize the specific site for the modification. Several experiments were performed using different

amounts of the Cx37 protein. Also, for a better identification of the possible modification site, different types of enzymes were used in mass spectrometry analysis. Unfortunately, the identification of modifications at the C-terminus of Cx37 was difficult as all enzymes cleaved the C-terminus at sites, making the analysis of the last 20 aa present in the C-terminus impossible. Due to this difficulty the analysis of Cx37 C-terminus with a possible site specific for posttranslational modifications could not be performed.

III.2 Characterization of Cx37GFP variants in HeLadel319 and HeLadel296 cells

III.2.1 Immunofluorescence staining of del319 and del296 in HeLadel319 and HeLadel296 cells

The expression of del319 and del296 in the cells was validated by immunofluorescence staining with Cx37 Ab using a confocal microscope. Figure III-12, depicts two cells (cell 1 and 2) each one showing an unstained distinct nucleus (N) and stained Cx37 at the contacts is the cells indicated by the arrow. The left panel shows the green fluorescence of GFP and the middle panel reveals Cx37 staining in red. The right panel depicts the overlay (yellow) of GFP fluorescence and Cx37 stained with the specific Ab. The overlay revealed the same location of GFP and Cx37 within the membrane of Cx37 mutant del319 and del296.

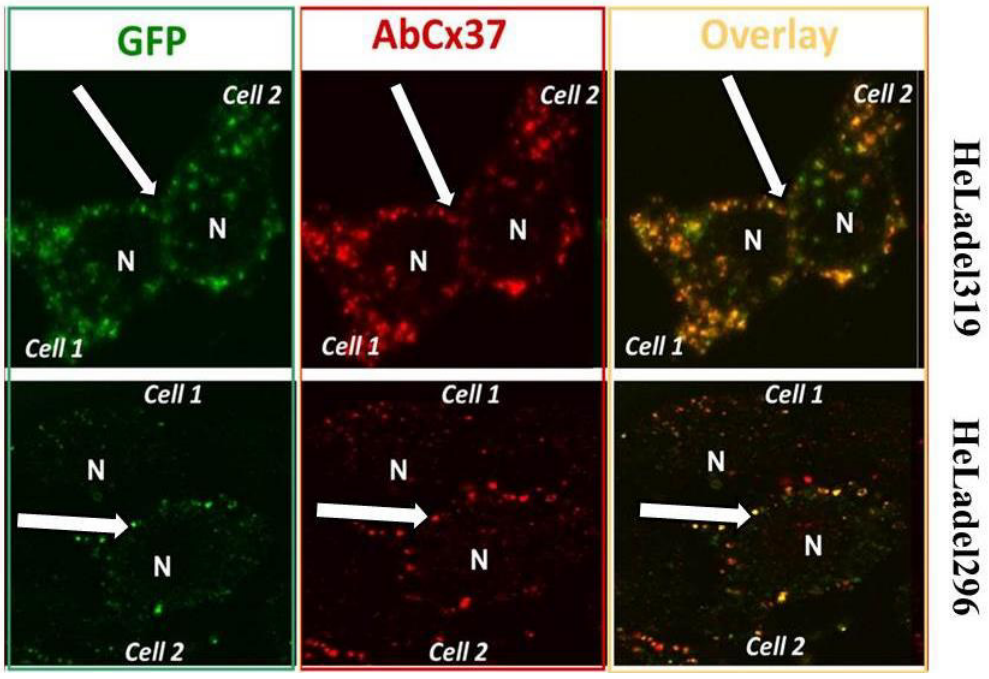

Figure III-12 Immunofluorescence staining revealed the same location of the GFP tag and Cx37 in the cells. The left panel represents the autofluorescence of GFP, the middle panel the staining with Cx37 Ab and the right panel the overlay of left and middle panels. The white arrows indicate the contact point between the cells.

III.2.2 Western Blot analysis of del319 and del296

SDS-Polyacrylamid gel electrophoresis followed by Western Blot analysis was used to observe the expression of del319 and del296 expression in corresponding cells. Figure III-13 depicts two Western Blots using specific antibodies (Abs) against GFP (Ab GFP, left blot) and Cx37 (Ab Cx37, right blot). For HeLadel319 a band at 63 kDa was observed and for HeLadel296 a band at 60 kDa was observed (black arrows Figure III-13).

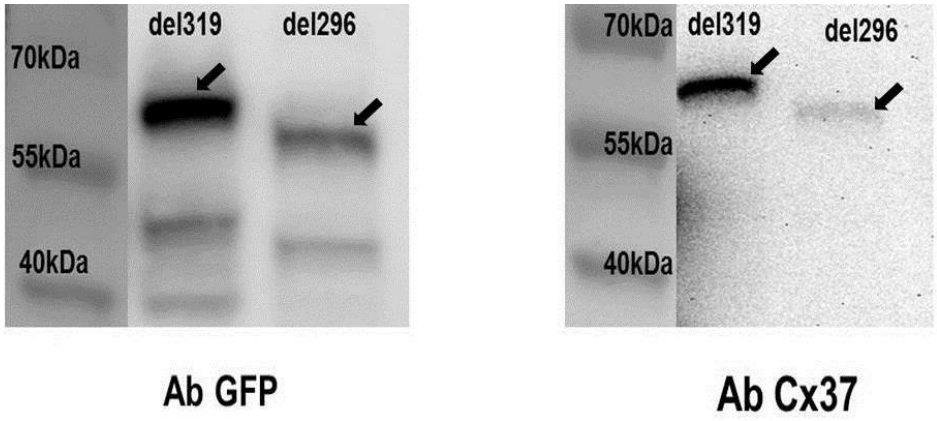

Figure III-13 del319 and del296 protein expression in HeLadel319 and HeLadel296 cells detected with Abs against Cx37 and GFP. The left blot with GFP Ab depicts the same bands as the right blot with the Cx37 Ab for del319 at 63 kDa and for del296 at 60 kDa.

III.2.3 mRNA expression of del319 and del296 mutants

The mRNA expression of the mutants was performed with the same primers used for Cx37GFP. In HeLadel319 and del296 cells three RT-PCR products were observed, one product at 741bp for GFP (indicated with a black arrow), one product at 288bp for Cx37 (indicated with a black arrow) and one product at 1580bp (part Cx37 and full GFP, indicated with a black arrow in Figure III-14). RT-PCR products observed in both mutants corresponded with the band size from control HeLa Cx37-, HeLa Cx43GFP- and also HeLa Cx37GFP-cells (see Figure III-4).

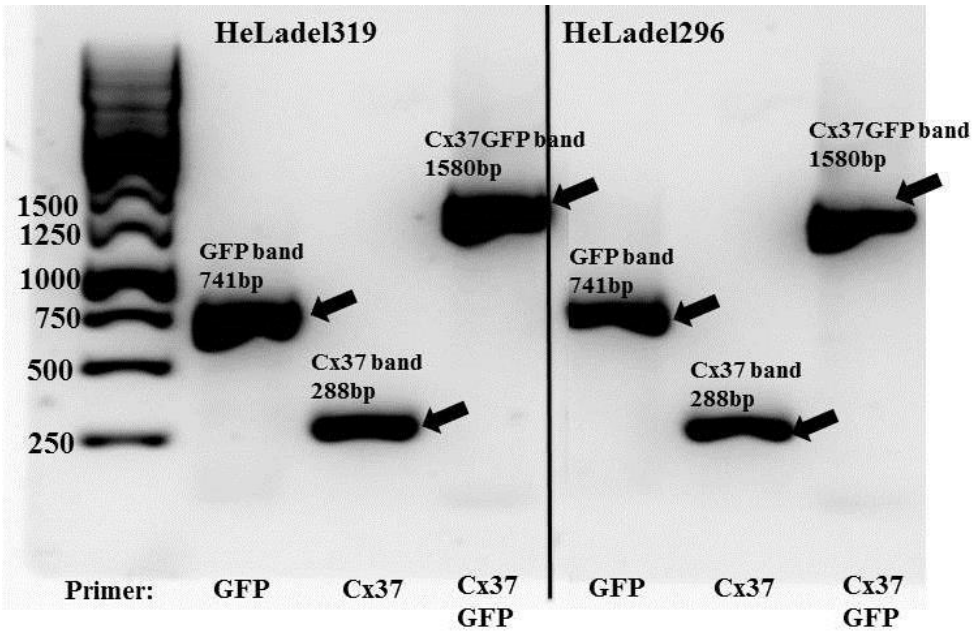

Figure III-14 RT-PCR products observed in HeLadel319 and HeLadel296 cells. HeLadel 319 and HeLadel296 revealed RT-PCR products at 288bp for Cx37, 741bp for GFP and 1580bp for part of Cx37 and full GFP. Similar products were observed in HeLa Cx37GFP cells.

III.2.4 Coupling of HeLadel319 and del296 cells and NO effect on mutants

The permeability of the GJs built by the Cx37 mutants del319 and del296 was analysed by detection of the intercellular calcium signaling induced by mechanical stimulation. Figure III-15 depicts that HeLadel296 and HeLadel319 could indeed form functional intact GJ channels. In non-treated HeLadel296 cells, calcium signal spread to 72±8 % (n=15, w=9, C=3) neighbouring cells, whereas HeLadel319 cells showed a lower number of coupled neighbouring cells (con: 48±5 %, n=27, w=12, C=6, Figure III-15 B). In contrast to full length HeLaCx37GFP, treatment of these cells with 2µM SNAP did not affect the intercellular calcium signal spreading (HeLadel296: NO: 64±7 %, n=15, w=11, C=3; HeLadel319: NO: 52±5 %, n=27, w=10, C=5). The results – compared with the full length experiments – showed that the 2µM SNAP effect was abolished in the mutants.

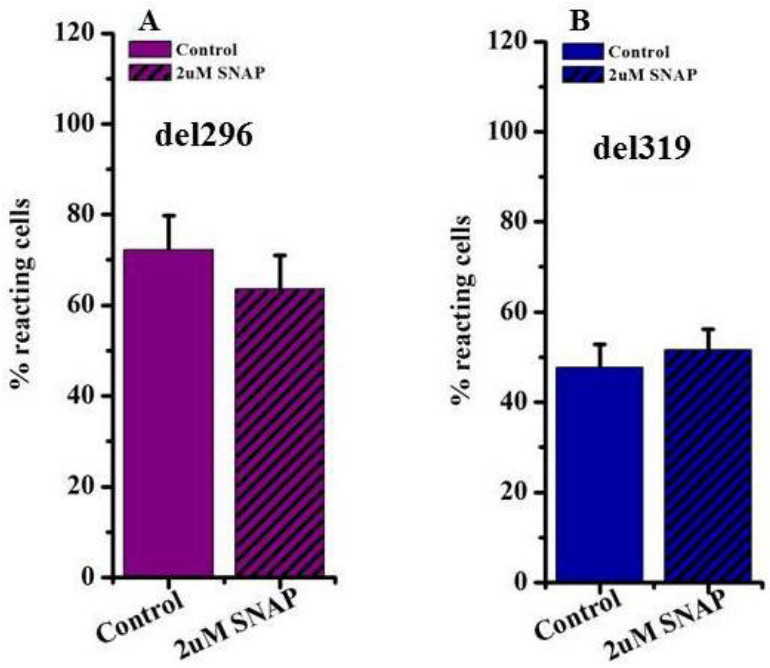

Figure III-15 Intercellular calcium signal spreading in HeLadel296 and HeLadel319. A depicts GJ coupling in del296 (Mann-Whitney test) and B depicts gap junction communication (GJC) in HeLadel319 cells(t-test). In both mutants, the SNAP effect on GJ coupling was no more observed.

III.2.5 The effect of pH 6.6 and H_2O_2 on HeLadel319 coupling

Furthermore, similarly as in full length Cx37-cells, experiments at a pH 6.6 and with 100mM H_2O_2 were performed for mutant HeLadel319. Figure III-16 A shows that at a pH of 7.4 58±8 % of the neighbouring cells were showing an increased calcium level upon stimulation. At a pH of 6.6 the GJ coupling was reduced to 24±7 % (n=14-16, w=7-9, C=3-5). In addition treatment with 100 mM H_2O_2 reduced GJ communication to 19±5 % versus control conditions 95 % (n=15-20, w=6-7, C=3, Figure III-16 B).

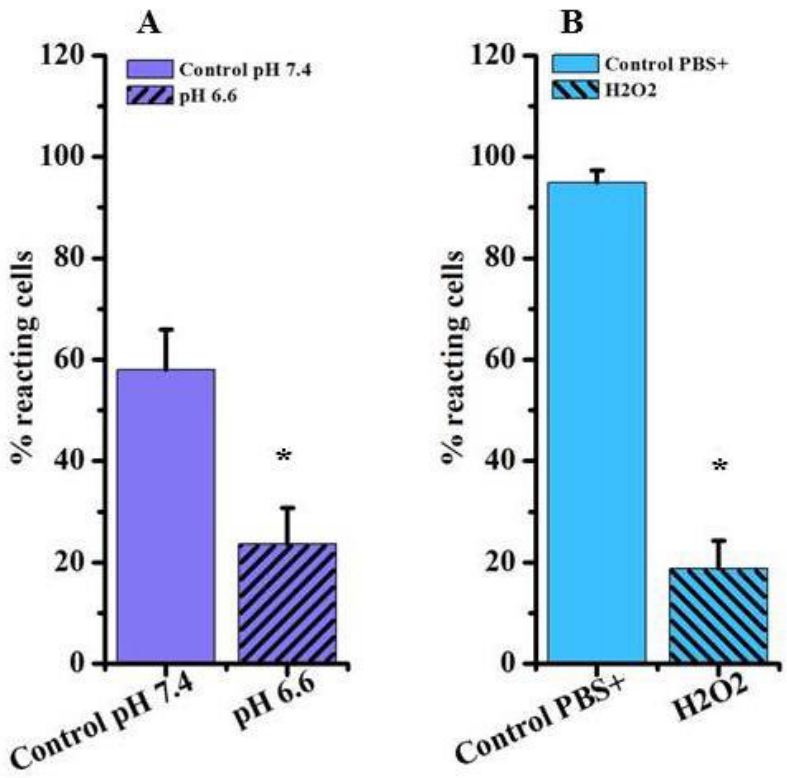

Figure III-16 Calcium signal spreading in HeLadel319 cells treated with pH 6.6 and 100 mM H_2O_2. Intercellular coupling of HeLadel319 cells was reduced by low pH 6.6 (A, Mann-Whitney test) and H_2O_2 (B, Mann-Whitney test).

III.2.6 The effect of genistein on HeLadel319 coupling

Figure III-17 depicts that 100µM genistein (a tyrosine kinases inhibitor) reduced the GJ coupling in HeLadel319 from control 99 % (n=13-15, w=6, C=3) to 86±4 %.

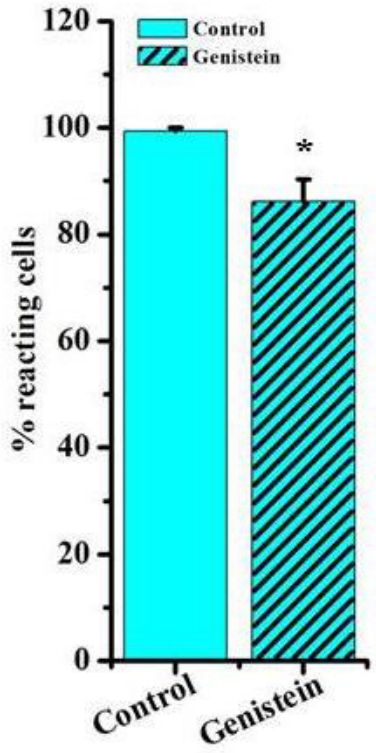

Figure III-17 Effect of genistein on GJ coupling in HeLadel319. Del319 control showed 99 % GJ coupling and 100µM genistein treatment reduced the coupling to 86±4 % (Mann-Whitney test).

III.3 Characterization of HeLaY332A cells

III.3.1 Immunofluorescence staining of HeLaY332A

Immunofluorescence assays were performed to analyse the localization of Y332A in the cells which was stably transfected in HeLa cells. Figure III-18 (left panel) depicts the localization of autofluorescent GFP which is found in the cytosol, in the cell membrane and also at the contact points between cells indicated by the arrow. The middle panel shows the immunohistochemical staining of GFP. The overlay picture (right panel) revealed the same location of GFP and mutant Cx37 in the plasma membrane of the cells (see white arrow).

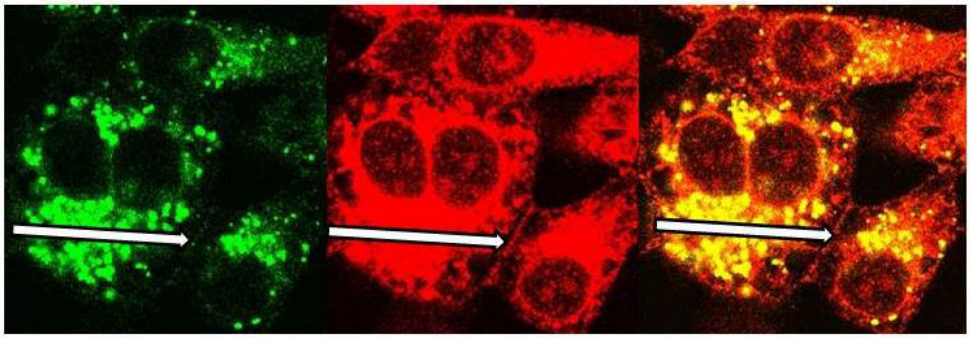

Figure III-18 Representative image of the GFP autofluorescence and specific GFP staining in HeLaY332A cells. The left panel represents the GFP autofluorescence, the middle panel the GFP Ab staining and the right panel the overlay of the left and right panel.

In addition, immunohistochemical analysis was also performed using Ab against Cx37 (middle panel Figure III-19). When overlaid with the transmission picture (right panel), the same location of the Y332A protein and the autofluorescent GFP (left panel) was found.

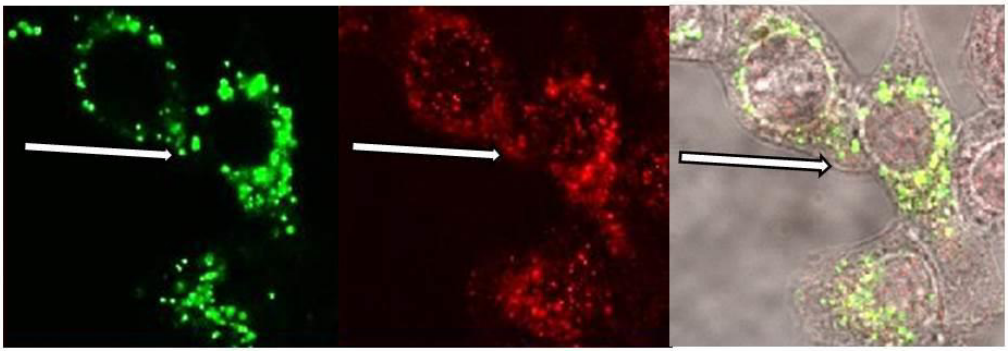

Figure III-19 Expression of Y332A in stably transfected HeLaY332A cells. The representative images show the autofluoresecence of GFP (left panel), immunhistochemical staining of Cx37 (the middle panel) and the overlay of both fluorescent images with the corresponding transmission image. The white arrows indicate the contact point between the cells.

III.3.2 Western Blot analysis and mRNA expression of point mutation Y332A

Figure III-20 depicts a Western Blot with HeLaY332A cells which revealed a protein band at 65 kDa.

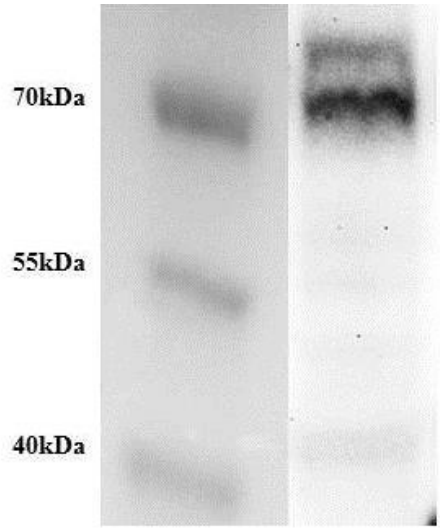

Figure III-20 The western blot with Cx37 Ab depicts a band at 65 kDa for HeLaY332A

In the next step, the mRNA was isolated from HeLaY332A and a RT-PCR was performed using the same primer as in experiments with other mutants. Figure III-21 depicts the RT-PCR gel with several bands: the left band at 741bp for the GFP part, the middle band at 288bp for the Cx37 and the right band for Cx37GFP at 1580bp (indicated by black arrows). All bands obtained had the same size as in full length Cx37GFP, mutant del319 and del296 cells.

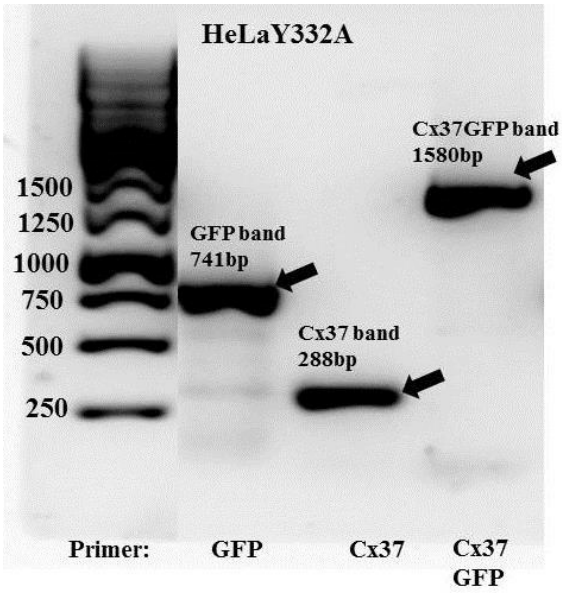

Figure III-21 RT-PCR products in HeLaY332A cells. The PCR products obtained from HeLaY332A had fragments with the size of 288 bp for Cx37, 741 bp for GFP and 1580bp for Cx37GFP.

III.3.3 Coupling of HeLaY332A cells and the effect of SNAP, pH 6.6 and 100mM H_2O_2 on mutant Y332A

The HeLaY332A cells expressing Cx37 with only one aa at position 332 exhibit a calcium signal transfer to 72±4 % of their neighbouring cells (n=14, w=5, C=2, Figure III-22 A). To test whether GJs formed by mutant Y332A could be blocked by SNAP or endogenous inhibitors the cells were incubated with 2 µM SNAP, pH 6.6 and 100 mM H_2O_2. 2 µM SNAP did not affect the intercellular communication (70±5 %, n=12, w=5, C=2) whereas pH 6.6 reduced the calcium signal transfer to 16±7 % (n=10, w=5, C=3) versus control pH 7.4 at 65±19 % (n=5, w=4, C=3; Fig. III-22 B). Figure III-22 C depicts that treatment with 100mM H_2O_2 showed a reduced calcium signal transfer at 10±5 % (n=11, w=4, C=2) compared with control (64±6 %, n=10, w=4, C=2). These results indicate that tyrosine at position 332 seems to be important for the mediation of the NO effect.

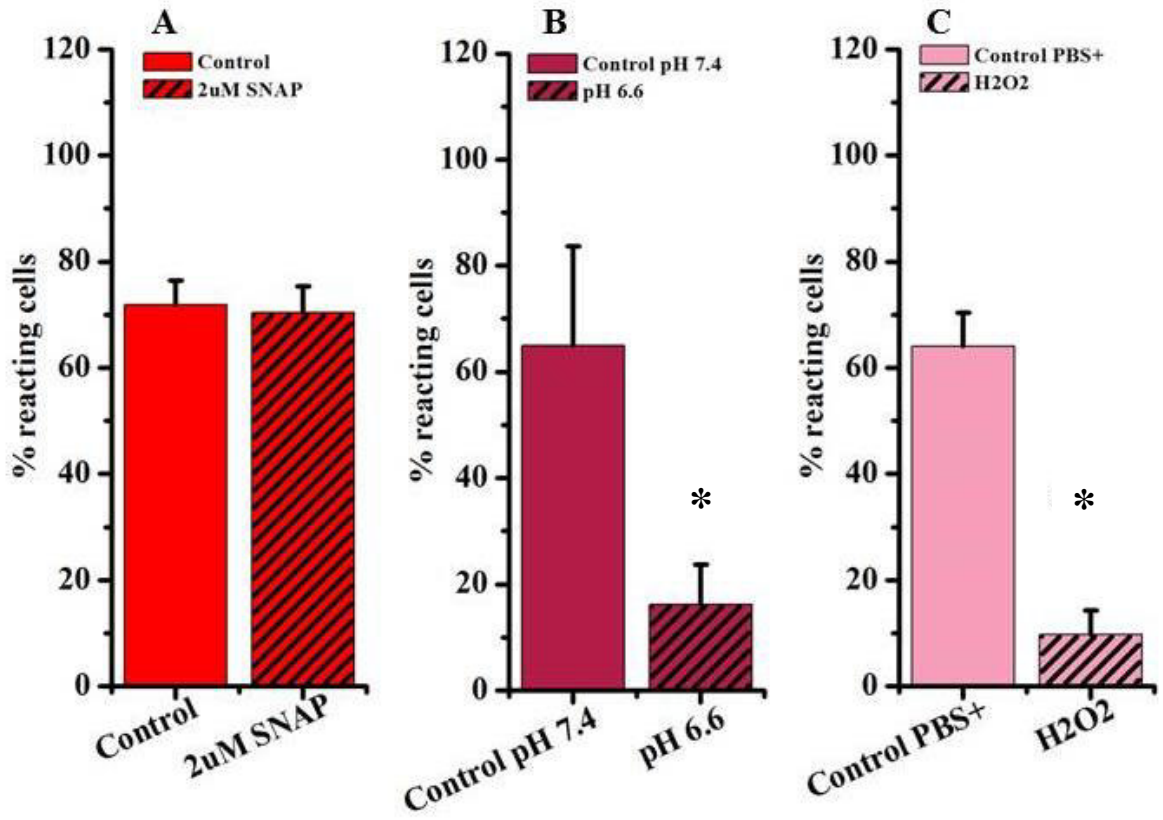

Figure III-22 GJ coupling in HeLaY332A cells after treatment with SNAP, pH6,6 and H_2O_2. A. GJ coupling under control conditions and after SNAP treatment (t-test). **B**. pH 7.4 conditions showed 65±19 % GJ coupling compared with 16±7 % at a pH of 6.6 (Mann-Whitney test). **C**. GJ coupling in control cells and after 100mM H_2O_2 treatment (Mann-Whitney test).

III.3.4 Effect of genistein on the GJ coupling in HeLaY332A cells

Finally, experiments with 100µM genistein were performed and revealed that genistein still reduced GJ communication from 81±6 % (con) to 50±6 % (genistein, n=11-14, w=5, C=3, Figure III-23).

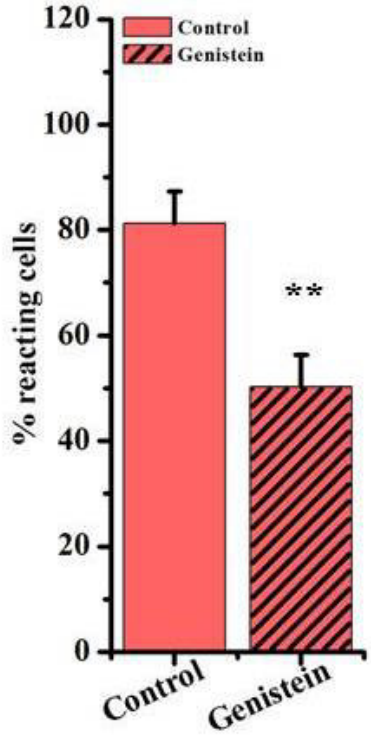

Figure III-23 GJ coupling of HeLaY332A cells treated with 100µM genistein. GJ communications was reduced after genistein treatment from 81±6 % to 50±6 % (t-test)

.

IV. DISCUSSION

In the present study we showed that Cx37GFP forms functionally intact GJs in HeLa cells, which allow the gap junctional calcium exchange to the same extent as wt-Cx37 do. The inhibitory effect of NO on the GJ calcium exchange, which is specific for Cx37, requires the presence of the last 19 aa in the C-terminus of Cx37 as assessed by the mutants del296 and del319. The lack of NO effects after conservative exchange of tyrosine 332 against alanine suggests that a NO mediated modification of this tyrosine forms the molecular basis of the NO mediated inhibition. This may be due to a change of tyrosine phosphorylation since the inhibitor of tyrosine phosphatases, orthovanadate, abolished the NO effect.

Our studies were performed in HeLa cells since their natural connexin genes are silenced (Cao et al., 1998) so that they do not express Cxs anymore in the wild type form in contrast to normal epithelial cells. This allows to study the effects of a defined connexin and of homotypic and homomeric gap junctions. This is important since, although in general molecules with a mass of less than 1kDa (sugars, amino acids, nucleotides, vitamins, ions and non-biological substances) can diffuse via GJs into neighbouring cells (Berg, 2013), the permeability of GJs is not uniform. The relative unitary conductance, in picoSiemens (pS) for homotypic channels is Cx37 (300pS) > Cx40 (140pS)> Cx43(100pS) > Cx45(30pS) (Johnstone et al., 2009). Several groups showed that different Cxs have a selective permeability to ions metabolites, fluorescent dyes and second messengers (IP_3, cAMP) (Elfgang et al., 1995; Weber, Chang, Spaeth, Nitsche, & Nicholson, 2004; Bedner et al., 2006). For example Cx43 have a high permeability for Alexa 488 compared with Alexa 350 (Weber et al., 2004). Bedner et al. showed that Cx43 is more permeable to cAMP than other Cxs (Cx26, Cx45 and Cx32) (Bedner et al., 2006). Homotypic gap junctions may rarely exist in cells such as endothelium or smooth muscle cells, which usually express several types of Cxs that may form heterotypic and heteromeric gap junctions. As a consequence, different permeabilities and also different regulation of permeability may result (Ek-Vitorin & Burt, 2013). It is therefore important to use a cell model which allows studying a certain connexin or a certain combination of connexins. The inhibitory effect of Cx37 is still functionally present, when hemichannels formed by Cx37 are coupling with hemichannels formed by Cx43. We have shown before, that at least the coupling between HeLa cells which express Cx43 and Cx37 and thus form heterotypic (but homomeric) gap junctions are still inhibitory regulated by NO (Kameritsch et al., 2005).

We have transfected HeLa cells with Cx37 and mutants of Cx37 which had been tagged with GFP. This GFP extended the C-terminus of Cx37. As already demonstrated by earlier findings of our laboratory, the addition of the GFP tag to Cx43 did neither affect its membrane distribution nor the channel functions of the respective gap junctions formed, as assessed by transfer of the small molecular dye calcein (J. Behrens, Kameritsch, Wallner, Pohl, & Pogoda, 2010). Here we could now show that the addition of GFP to the Cx37 protein did also not affect

its membrane distribution or calcium permeability when compared to wt Cx37. This was also true for the mutants we have used. Thus, the modification with GFP did not functionally affect gap junctional coupling. Similar results were also reported by Kyle et al. who used transient transfected HeLa cells with GFP-tagged Cx37 to study the membrane distribution and permeability of mutations of the N-terminus (Kyle et al., 2008). These authors also report a functional channel formation with full length, GFP tagged Cx37 (Kyle et al., 2009). The tag allowed the use of GFP antibodies and GFP nanobeads for a better analysis of Cx37 and its mutants with regard to localization and expression. Expression of GFP tagged Cx37 has also been shown by Western blot using GFP antibodies. Cx37 showed a band at around 37 kDa (A. Harris, 2009). It its known, that GFP has 28 kDa and in our experiments cells revealed bands for Cx37GFP del319 at 63kDa, Cx37GFP del296 at 60 kDa and Cx37GFPY332A at 65 kDa. All mutants had size bands corresponding to their predicted molecular mass. Cx37GFP showed a band at 55 kDa which was lower than the expected value of 65 kDa. As the RT-PCR led to the correct DNA fragment and the connexins were inserted into the membrane forming functional gap junctions comparable to Cx37 we used the HeLaCx37GFP in our experiments despite the wrong size in the western blot.. GFP mutants of connexins were also shown to be functional. E.g. Hunter et al. used GFP tagged Cx43 in their experiments and they showed that GJ plaques were formed even if ZO-1 is not binding to Cx43-GFP (Hunter, Jourdan, & Gourdie, 2003). Breidert et al. used a GFP tagged Cx49 to observe the intracellular transport and traffic of Cx43-GFP. Their study provides new information about Cx transport to the plasma membrane, GJ formation and which elements could be involved in Cxs sorting and which proteins are involved in Cx folding (Breidert, Jacob, Ngezahayo, Kolb, & Naim, 2005).

In this study we assessed the gap junctional transfer of calcium or calcium releasing agents as derived from calcium increases in adjacent cells after mechanical stimulation of a single cell. Mechanical stimulation leads also to the release of ATP via hemichannels, which could also lead to calcium increases in neighbouring cells by acting on P2 receptors. This paracrine stimulation was excluded by treating the cells with a purinergic P2 receptor blocker, suramin (Hoyle, Knight, & Burnstock, 1990), which blocked the direct action of exogenously applied ATP up to a concentration above 10 µM. Indeed we did not observe a calcium increase in the neighbourhood of mechanically stimulated wt HeLa cells lacking connexins. This further supports our view, that the induction of calcium increases in neighbouring cells was GJ dependent and, therefore, a measure of gap junctional coupling and – indirectly – of their overall permeability. The mechanical stimulation of a single cell led to an increase in cytosolic calcium, probably due to an activation of some of its mechanosensitive calcium channels. Previous experiments of others and our own laboratory yielded evidence that the gap junctional transfer to adjacent cells involves calcium as well as IP_3, the latter being important for eliciting calcium responses in remote cells (Kameritsch et al., 2012). Our experiments revealed that all mutants studied showed functional GJ coupling. The variations in the number of cells reacting did not indicate any systemic reduction of the gap junctional permeability to calcium in the mutant cells. It must be emphasized that the number of reacting cells is only an indirect measure of calcium

permeability of gap junctions and depends also on other variables such as the confluence of cells and local geometric conditions.

Nevertheless, our experiments clearly showed that exogenous NO, as generated by the treatment with the NO donor SNAP (Kameritsch et al., 2005), showed a reproducible and highly significant reduction of gap junctional calcium transfer. This inhibitory effect was dose dependent. Previous calculations suggest that the standard dose used here may well relate to the high normal concentration range of NO that is achieved during pharmacologic endothelial cell stimulation. The treatments of cells with 1 µM SNAP correspond to a local concentration of about 2 nM NO (Ishida et al., 1996) therefore the NO used in experiments can be calculated to be around 100 pM up to approximately 5 nM as pointed out by Kameritsch et al. in their recent paper. This is a concentration range reached during endothelial cell stimulation (Hall & Garthwaite, 2009).

We have shown before that NO also blocks the gap junctional transfer of molecules of higher mass such as Alexa Fluor 488, calcein or carboxyfluorescein (Kameritsch et al., 2005) suggesting that also the transfer of cyclic nucleotides which have a similar molecular mass and surface charge may be compromised. However, we have also shown before that the electrical coupling, which is carried by ions is not significantly affected by NO (Kameritsch et al., 2005) which can be explained by the relative concentrations of calcium as compared to other anions and cations such as chloride, potassium and sodium. Our observations are in line with others reporting NO inhibitory effects on Cx37 in microvascular endothelial cells (McKinnon et al., 2009). In neuronal cells, GJ permeability was reduced by NO via cGMP (Rorig & Sutor, 1996) and similar results were observed in cardiac cells (Kwak & Jongsma, 1996). Vasoconstriction in mouse cremaster arterioles was diminished by NO (endogenous and exogenous) but involved other Cxs than Cx40 (Rodenwaldt, Pohl, & de Wit, 2007). Interestingly Pfenninger et al. demonstrated in EC an interaction between eNOS and Cx37 (Pfenniger et al., 2010). Straub et al. showed in vitro model of co-cultured EC and SMC that MEJ communication was enhanced by NO and also found that eNOS and Cx43 are present in MEJ (Straub et al., 2011). However, our results do not require a direct interaction of the connexin and NOS. Moreover, no acute inhibitory effects of NO on cells being coupled with Cx43 homotypic GJs were observed (not shown).

Interestingly, NO is involved in the permeability control of another endothelial connexin, Cx40. Hoffmann et al. have shown that NO can enhance the de novo formation of endothelial GJs, thereby enhancing gap junction permeability for calcein (Hoffmann, Gloe, Pohl, & Zahler, 2003). This effect was mediated by a PKA mediated phosphorylation of Cx40, NO increasing the cAMP level of endothelial cells by its inhibitory effects on cAMP degrading phosphodiesterases (Hoffmann et al., 2003). In contrast to the effect of NO on Cx37, this is a delayed effect which requires minutes to hours, whereas the effect of NO on Cx37 occurs within seconds (Hoffmann et al., 2003).

One of the aims of this study was to analyse how NO could modify the Cx37 protein so that a reduction of Cx37 containing gap junctions could occur.

GJ channels can open and close in a very dynamic way. There are two models how this change can occur – the ball and chain model (Delmar, Coombs, Sorgen, Duffy, & Taffet, 2004), and a model that suggests a small rotation of each subunit which accordingly may result in opening or closing the channel (Alberts, 2002). Figure IV-1 depicts the latter model showing schematically the response of the channel conformation to changes of pH or local calcium concentration (Alberts, 2002).

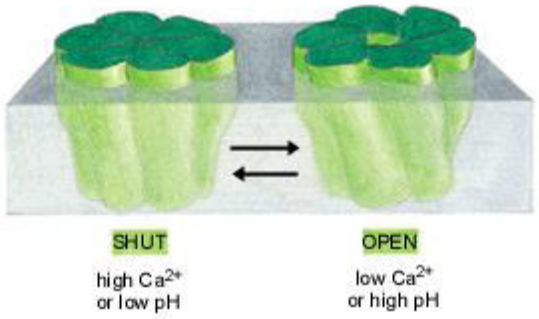

Figure IV-1 Proposed model for changes of GJ channel permeability in response to changes in Ca^{2+} or pH in the cytosol. Picture modified after (Alberts, 2002).

Alternatively a "ball-and-chain" or "particle-receptor" model (Figure IV-2) was proposed e.g. as a mechanism leading to reduced permeability following intracellular acidification inducing GJ closing (Delmar et al., 2004; Ek-Vitorin et al., 1996; Stergiopoulos et al., 1999). This model suggests that the "ball" or "particle" (C-terminus domain of Cx) interacts directly with the "receptor" or "chain" (intercellular loop S255 - A311) in order to close the GJ channels.

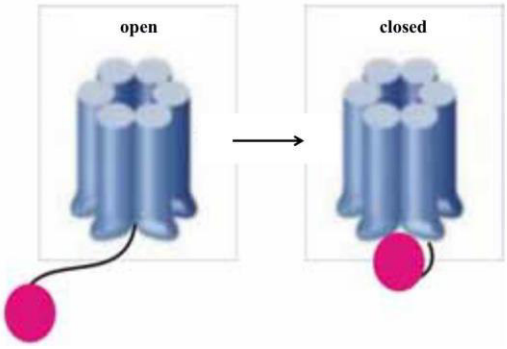

Figure IV-2 Scheme of the "ball-and-chain" model that closes GJ channels. The ball is formed by the C-terminus domain and binds to the intracellular loop "receptor" domain. For clarity, only one ball and chain forming a hemichannel are indicated on the figure. Picture taken from (Delmar et al., 2004).

The interaction between the C-terminus domain and the cytoplasmic loop is thought to be regulated by modifications of the cytoplasmatic C-terminus loop of the connexins (A. L. Harris, 2001). The best known modifications are phosphorylations. In Cx 43, about 14 potential

phosphorylation sites are considered to exist (Lampe & Lau, 2004; Marquez-Rosado, Solan, Dunn, Norris, & Lampe, 2012; Solan & Lampe, 2009), similar numbers are reported for Cx37 (Burt et al., 2008; Traub et al., 1998). The sequence homology of the Cx37 C-terminus and the Cx43 C-terminus could suggest the following similar binding sites: for MAPK Cx43-Ser282 and Cx37-Ser275 and for PKC Cx43-Ser368 and Cx37-Ser282 (Burt et al., 2008). It is known that Cx43 has in the C-terminus 2-6 tyrosine phosphorylation sites and that tyrosine phosphorylation of Cx43 decreases the GJ permeability (Goodenough, Goliger, & Paul, 1996)

Several groups have shown that mouse Cx37 can be phosphorylated at serine and – to a smaller extent - at tyrosine and threonine residues (Traub et al., 1998); the kinases implicated in this process were not identified (Larson et al., 2000). Moreover, Morel et al. showed that the region around the polymorphic position 319 of Cx37 C-terminus could be a site for phosphorylation for glycogen synthase kinase-3 (GSK-3) (Morel et al., 2010). Another group showed that there are two polymorphic mutants of Cx37 existing in the human population one expressing a serine (Cx37-S319 which can be phosphorylated) and the other a proline (P/Pro) (Cx37-P319 which cannot be phosphorylated) at position 319 (C-terminus) and it could be shown that a correlation of Cx37-P319 with an increased incidence of atherosclerosis exists (Boerma et al., 1999; Pfenniger et al., 2010).

We therefore tried to identify which region of the C-terminus might be involved in the NO dependent regulation of the permeability of Cx37 containing gap junction channels. The C-terminus of Cx37 has serine, cysteine and tyrosine residues which are potentially subject to a posttranslational modification. To determine the specific site of the Cx37GFP modifications induced by NO, we created mutant cells in which Cx37 consisting of 333 aa (without GFP) was shortened at the C-terminus by 14 aa (del319), or 37 aa (del296). As pointed out already, these mutants showed normal incorporation into the cell membrane and no quantifiable alteration of their GJ calcium permeability. However, the inhibitory effect of NO on GJ calcium permeability was lost in these cells. This was not an unspecific effect of the mutation, since the inhibition by H_2O_2 or low pH was still present and unaltered. Moreover, the use of two different mutants showing the same result minimize further the risk that the lack of NO dependent inhibition was due to unspecific conformational changes which is always inherent in such deletion experiments. A sequence analysis of the C-terminus yielded only one tyrosine residue in the deleted terminal region which could be subject to NO induced phosphorylation or nitrosylation. Figure IV-3 shows the polypeptide sequence of Cx37GFP schematically, black color representing the N-terminus, yellow the 4 transmembrane domains, blue the two extracellular loops, purple the cytoplasmic loop cytosolic located, red the C-terminus, gray the spacer and green GFP. Several tyrosine residues are present in Cx37 sequence (pink Y in Figure IV-3), the C-terminus (red sequence) has 4 tyrosine (black arrows) and for the final 14 aa one tyrosine can be identified.

Figure IV-3 Polypeptide sequence of Cx37GFP were tyrosine residues are present. C-terminus with 4 tyrosine indicated by the black arrows and only one tyrosine observed in the last 14 aa.

Therefore, in a further step, this tyrosine at position 332 was exchanged by alanine (Y332A). The experiments with the point mutation Y332A showed, that the NO effect was lost though the C-terminus length was not altered in this case. These results indicate that the presence of Y332 is an essential prerequisite for NO induced control of Cx37 dependent gap junctional permeability. To our knowledge, this is the first study which indicates a specific C-terminus site for NO effect in Cx37.

NO could modify the tyrosine target directly or indirectly by several independent mechanisms: Firstly, it could exert its effect by an activation of guanylyl cyclase and the downstream cGMP pathway. NO is well known binding to the heme group of soluble guanylyl cyclase which is present in many cells thereby eliciting the enhanced formation of the second messenger 3`-5`cyclic guanosine monophosphate (cGMP) (Francis et al., 2010; Munzel et al., 2003). An important downstream kinase is the protein kinase G (PKG) (Johnstone et al., 2009), which can phosphorylate target proteins. However, the PKG is a Ser / Thr kinase which could not directly phosphorylate the tyrosine residue identified here as a potential target. Moreover, we have shown before that the effect of NO on Cx37 is cGMP independent, since treatment with the sCG inhibitor ODQ (Kameritsch et al., 2005) did not prevent the effect of NO. However, there are a plethora of other enzymes, including tyrosine kinases or phosphatases, which could be activated by NO e.g. through S-nitrosylation and secondarily control the phosphorylation of Y332.

Reactive cysteine thiols and NO form covalently S-nitrosothiol groups (Lima, Forrester, Hess, & Stamler, 2010). Most cGMP independent effects of NO are thought to be mediated via S-nitrosylation (Lima et al., 2010), which can induce protein modifications. Our S-nitrosylation assay experiments showed differences between control and SNAP treatment. The difference suggests that Cx37GFP could be S-nitrosylated in the presence of NO but the specific location of these modifications could not be localized further. Figure IV-4 depicts the localization of Cys residues (represented in dark blue) within the peptide sequence of Cx37GFP with following: black color representing the N-terminus, yellow the 4 transmembrane domains with one Cys, purple the cytoplasmic loop, blue the two extracellular loops with 5 Cys, grey the spacer without Cys, red the C-terminus with 3 Cys and green the GFP (green) with 3 Cys.

Figure IV-4 Cysteine residues observed in the Cx37GFP polypeptide sequence. 13 cysteine residues are present in Cx37GFP sequence. Cx37 has 10 Cys with 3 Cys located in the C-terminus and 3 Cys in GFP.

However, del319 and del296 mutants which show a loss of NO effect have no Cys in this part of the C-terminus which makes a role for S-nitrosylation in our context unlikely.

Finally, NO can react with superoxide to form peroxynitrite (Pacher, Beckman, & Liaudet, 2007). Peroxynitrite (ONOO-) is known e.g. to activate Mitogen activated protein kinase (MAPKs) and other enzymes (Liaudet, Vassalli, & Pacher, 2009). MAPK are, however, again Ser /Thr Kinases (Cargnello & Roux, 2011) which may, however, not directly affect Y332.

Within the time constraints of this thesis it was not possible to analyse the modification of Y332 by mass spectrometry. While the results revealed the presence of Cx37 posttranslational modifications the final region of the C-terminus could not be analysed as the respective protein fragments could not be sufficiently recovered after treatment with several standard enzyme mixtures. The most common modification of tyrosine is phosphorylation. Moreover, we did also not find in western blot experiments distinct differences in the overall phosphorylation of Cx37GFP. However, the complete C-terminus of Cx37 contains four different tyrosine residues the variable phosphorylation of which could have masked changes in Y332.

However, pretreatment with an inhibitor of tyrosine phosphatases, orthovanadate also abolished the NO effect. This suggests that NO may affect the activity of a tyrosine phosphatase and thereby indirectly control the phosphorylation at Y332. However, orthovanadate is not fully specific and can also affect the effect of ATPases (Pezza, Villarreal, Montich, & Argaraña, 2002) which limits the interpretability of our results. At first glance, the inhibitory effects of genistein, a tyrosine kinase inhibitor, on the NO effect would support the idea that NO interfered with the phosphorylation state of Y332. Unfortunately, genistein also reduced the calcium permeability of gap junctions formed by the Y332A mutant, pointing to the fact that genistein probably affects many phosphorylation processes in the cell.

Our study confirmed that NO inhibits GJ communication between cells when Cx37 is involved. While we identify for the first time a specific amino acid residue of its C-terminus, Y332 as being essential for this effect, it was not designed to clarify the functional significance of the Cx37 dependent inhibitory effect of NO. This would be necessary to decide whether the

phosphorylation state of Y332 would be a potential therapeutic target and what the consequences of an impaired NO production or availability were on gap junctional communication. However, recent findings by our laboratory (Pogoda et al., 2014) may shed some light on the potential significance. Pogoda et al. showed that NO has effect on bidirectional GJ communication (GJC) between EC and SMC in co-culture and also that endothelial Cx37 are located within the internal elastic lamina very close to smooth muscle Cx43.

For these reasons, we propose a functional consequence for the NO effect on MEGJ (Figure IV-5). Stimulation of EC leads to an increase of intracellular Ca^{2+}concentration, which can pass to the neighbouring EC cells via EC GJ (acting as one functional unit) or can diffuse to the underlying VSM. At the same time, more nitric oxide (NO) is produced by EC, which reduces the calcium loss to VSM. As a consequence, calcium increases in EC, which is essential for endothelial autacoid synthesis and may be augmented and prolonged (Pogoda et al. 2014) thereby, augmenting the endothelial influence on vascular tone.

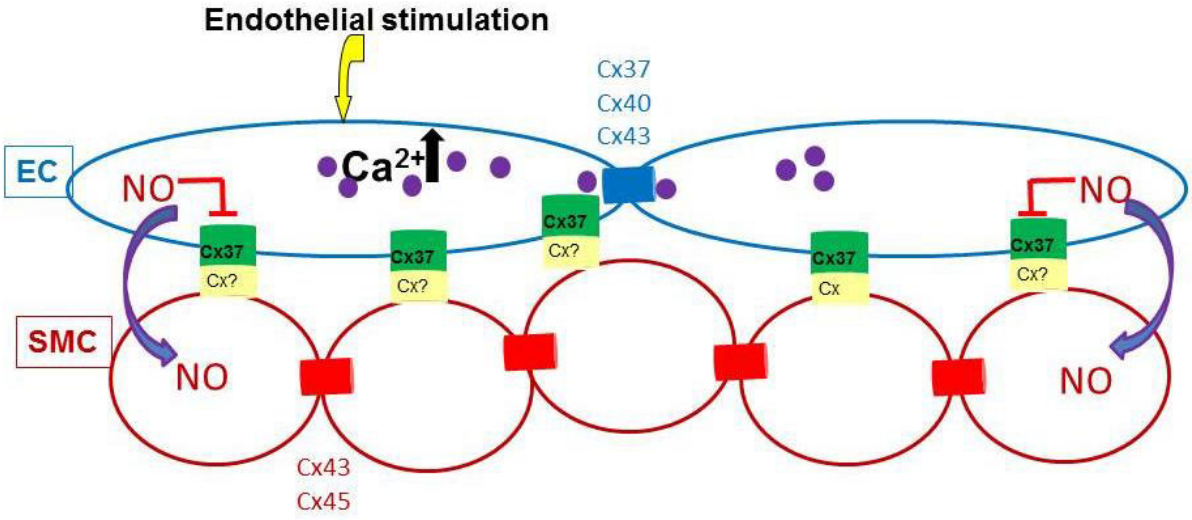

Figure IV-5 The effect of NO on MEGJ communication depicts that NO, produced by the EC, diffuses to the SMC and produces SMC relaxation. Furthermore, at the same it blocks Cx37- containing MEGJ preventing a Ca^{2+}loss from EC to SMC and therefore increasing the endothelial response to stimulation.

V. REFERENCES

Alberts, B. (2002). *Molecular biology of the cell* (4. ed. ed.). New York, NY [u.a.]: Garland.

Bedner, P., Niessen, H., Odermatt, B., Kretz, M., Willecke, K., & Harz, H. (2006). Selective permeability of different connexin channels to the second messenger cyclic AMP. *J Biol Chem, 281*(10), 6673-6681. doi: 10.1074/jbc.M511235200

Behrens, J., Kameritsch, P., Wallner, S., Pohl, U., & Pogoda, K. (2010). The carboxyl tail of Cx43 augments p38 mediated cell migration in a gap junction-independent manner. *Eur J Cell Biol, 89*(11), 828-838. doi: 10.1016/j.ejcb.2010.06.003

Behrens, J. V. (2011). A channel independent function of connexin 43 in cell migration.

Berg, J. M. S. (2013). *Biochemistry*.

Boerma, M., Forsberg, L., Van Zeijl, L., Morgenstern, R., De Faire, U., Lemne, C., Cotgreave, I. A. (1999). A genetic polymorphism in connexin 37 as a prognostic marker for atherosclerotic plaque development. *J Intern Med, 246*(2), 211-218.

Breidert, S., Jacob, R., Ngezahayo, A., Kolb, H. A., & Naim, H. Y. (2005). Trafficking pathways of Cx49-GFP in living mammalian cells. *Biol Chem, 386*(2), 155-160. doi: 10.1515/bc.2005.019

Bright, G. R., Fisher, G. W., Rogowska, J., & Taylor, D. L. (1989). Fluorescence ratio imaging microscopy. *Methods Cell Biol, 30*, 157-192.

Burt, J. M., Nelson, T. K., Simon, A. M., & Fang, J. S. (2008). Connexin 37 profoundly slows cell cycle progression in rat insulinoma cells. *Am J Physiol Cell Physiol, 295*(5), C1103-1112. doi: 10.1152/ajpcell.299.2008

Cannon, R. O., 3rd. (1998). Role of nitric oxide in cardiovascular disease: focus on the endothelium. *Clin Chem, 44*(8 Pt 2), 1809-1819.

Cao, F., Eckert, R., Elfgang, C., Nitsche, J. M., Snyder, S. A., DF, H. u., Nicholson, B. J. (1998). A quantitative analysis of connexin-specific permeability differences of gap junctions expressed in HeLa transfectants and Xenopus oocytes. *J Cell Sci, 111 (Pt 1)*, 31-43.

Cargnello, M., & Roux, P. P. (2011). Activation and function of the MAPKs and their substrates, the MAPK-activated protein kinases. *Microbiol Mol Biol Rev, 75*(1), 50-83. doi: 10.1128/mmbr.00031-10

Dbouk, H. A., Mroue, R. M., El-Sabban, M. E., & Talhouk, R. S. (2009). Connexins: a myriad of functions extending beyond assembly of gap junction channels. *Cell Commun Signal, 7*, 4. doi: 10.1186/1478-811x-7-4

de Wit, C., & Griffith, T. M. (2010). Connexins and gap junctions in the EDHF phenomenon and conducted vasomotor responses. *Pflugers Arch, 459*(6), 897-914. doi: 10.1007/s00424-010-0830-4

de Wit, C., Roos, F., Bolz, S. S., Kirchhoff, S., Kruger, O., Willecke, K., & Pohl, U. (2000). Impaired conduction of vasodilation along arterioles in connexin40-deficient mice. *Circ Res, 86*(6), 649-655.

Delmar, M., Coombs, W., Sorgen, P., Duffy, H. S., & Taffet, S. M. (2004). Structural bases for the chemical regulation of Connexin43 channels. *Cardiovasc Res, 62*(2), 268-275. doi: 10.1016/j.cardiores.2003.12.030

Duffy, H. S., Delmar, M., & Spray, D. C. (2002). Formation of the gap junction nexus: binding partners for connexins. *J Physiol Paris, 96*(3-4), 243-249.

REFERENCES

Ek-Vitorin, J. F., & Burt, J. M. (2013). Structural basis for the selective permeability of channels made of communicating junction proteins. *Biochim Biophys Acta, 1828*(1), 51-68. doi: 10.1016/j.bbamem.2012.02.003

Ek-Vitorin, J. F., Calero, G., Morley, G. E., Coombs, W., Taffet, S. M., & Delmar, M. (1996). PH regulation of connexin43: molecular analysis of the gating particle. *Biophys J, 71*(3), 1273-1284. doi: 10.1016/s0006-3495(96)79328-1

Elfgang, C., Eckert, R., Lichtenberg-Frate, H., Butterweck, A., Traub, O., Klein, R. A., Willecke, K. (1995). Specific permeability and selective formation of gap junction channels in connexin-transfected HeLa cells. *J Cell Biol, 129*(3), 805-817.

Figueroa, X. F., & Duling, B. R. (2009). Gap junctions in the control of vascular function. *Antioxid Redox Signal, 11*(2), 251-266. doi: 10.1089/ars.2008.2117

Figueroa, X. F., Isakson, B. E., & Duling, B. R. (2004). Connexins: gaps in our knowledge of vascular function. *Physiology (Bethesda), 19*, 277-284. doi: 10.1152/physiol.00008.2004

Francis, S. H., Busch, J. L., Corbin, J. D., & Sibley, D. (2010). cGMP-dependent protein kinases and cGMP phosphodiesterases in nitric oxide and cGMP action. *Pharmacol Rev, 62*(3), 525-563. doi: 10.1124/pr.110.002907

Giepmans, B. N. (2004). Gap junctions and connexin-interacting proteins. *Cardiovasc Res, 62*(2), 233-245. doi: 10.1016/j.cardiores.2003.12.009

Goodenough, D. A., & Gilula, N. B. (1974). The splitting of hepatocyte gap junctions and zonulae occludentes with hypertonic disaccharides. *J Cell Biol, 61*(3), 575-590.

Goodenough, D. A., Goliger, J. A., & Paul, D. L. (1996). Connexins, connexons, and intercellular communication. *Annu Rev Biochem, 65*, 475-502. doi: 10.1146/annurev.bi.65.070196.002355

Goodenough, D. A., & Paul, D. L. (2009). Gap junctions. *Cold Spring Harb Perspect Biol, 1*(1), a002576. doi: 10.1101/cshperspect.a002576

Haddock, R. E., Grayson, T. H., Brackenbury, T. D., Meaney, K. R., Neylon, C. B., Sandow, S. L., & Hill, C. E. (2006). Endothelial coordination of cerebral vasomotion via myoendothelial gap junctions containing connexins 37 and 40. *Am J Physiol Heart Circ Physiol, 291*(5), H2047-2056. doi: 10.1152/ajpheart.00484.2006

Haefliger, J. A., Krattinger, N., Martin, D., Pedrazzini, T., Capponi, A., Doring, B., Meda, P. (2006). Connexin43-dependent mechanism modulates renin secretion and hypertension. *J Clin Invest, 116*(2), 405-413. doi: 10.1172/jci23327

Hall, C. N., & Garthwaite, J. (2009). What is the real physiological NO concentration in vivo? *Nitric Oxide, 21*(2), 92-103. doi: 10.1016/j.niox.2009.07.002

Harris, A. (2009). *Connexins a guide*. New York: Humana Press.

Harris, A. L. (2001). Emerging issues of connexin channels: biophysics fills the gap. *Q Rev Biophys, 34*(3), 325-472.

Hill, C. E., Rummery, N., Hickey, H., & Sandow, S. L. (2002). Heterogeneity in the distribution of vascular gap junctions and connexins: implications for function. *Clin Exp Pharmacol Physiol, 29*(7), 620-625.

Hirst, R. A., Harrison, C., Hirota, K., & Lambert, D. G. (1999). Measurement of $[Ca^{2+}]i$ in whole cell suspensions using fura-2. *Methods Mol Biol, 114*, 31-39. doi: 10.1385/1-59259-250-3:31

Hoffmann, A., Gloe, T., Pohl, U., & Zahler, S. (2003). Nitric oxide enhances de novo formation of endothelial gap junctions. *Cardiovasc Res, 60*(2), 421-430.

Hoyle, C. H., Knight, G. E., & Burnstock, G. (1990). Suramin antagonizes responses to P2-purinoceptor agonists and purinergic nerve stimulation in the guinea-pig urinary bladder and taenia coli. *Br J Pharmacol, 99*(3), 617-621.

Hunter, A. W., Jourdan, J., & Gourdie, R. G. (2003). Fusion of GFP to the carboxyl terminus of connexin43 increases gap junction size in HeLa cells. *Cell Commun Adhes, 10*(4-6), 211-214.

Isakson, B. E., Best, A., & Duling, B. R. (2008). Incidence of protein on actin bridges between endothelium and smooth muscle in mouse arterioles demonstrates heterogeneous connexin expression and phosphorylation. *Am J Physiol Heart Circ Physiol, 294*(6), H2898-2904.

Isakson, B. E., & Duling, B. R. (2005). Heterocellular contact at the myoendothelial junction influences gap junction organization. *Circ Res, 97*(1), 44-51. doi: 10.1161/01.RES.0000173461.36221.2e

Ishida, Y., Hashimoto, M., Fukushima, S., Masumura, S., Sasaki, T., Nakayama, K., Momose, K. (1996). A nitric oxide-sensitive electrode: requirement of lower oxygen concentration for detecting nitric oxide from the tissue. *J Pharmacol Toxicol Methods, 35*(1), 19-24.

Johnstone, S., Isakson, B., & Locke, D. (2009). Biological and biophysical properties of vascular connexin channels. *Int Rev Cell Mol Biol, 278*, 69-118. doi: 10.1016/s1937-6448(09)78002-5

Kameritsch, P., Hoffmann, A., & Pohl, U. (2003). Opposing effects of nitric oxide on different connexins expressed in the vascular system. *Cell Commun Adhes, 10*(4-6), 305-309.

Kameritsch, P., Khandoga, N., Nagel, W., Hundhausen, C., Lidington, D., & Pohl, U. (2005). Nitric oxide specifically reduces the permeability of Cx37-containing gap junctions to small molecules. *J Cell Physiol, 203*(1), 233-242. doi: 10.1002/jcp.20218

Kameritsch, P., Pogoda, K., Ritter, A., Munzing, S., & Pohl, U. (2012). Gap junctional communication controls the overall endothelial calcium response to vasoactive agonists. *Cardiovasc Res, 93*(3), 508-515. doi: 10.1093/cvr/cvr345

Korthuis, R. J. (2011). *Skeletal Muscle Circulation*. San Rafael CA: 2011 by Morgan & Claypool Life Sciences.

Kumar, N. M., & Gilula, N. B. (1996). The gap junction communication channel. *Cell, 84*(3), 381-388.

Kurjiaka, D. T., & Segal, S. S. (1995). Conducted vasodilation elevates flow in arteriole networks of hamster striated muscle. *Am J Physiol, 269*(5 Pt 2), H1723-1728.

Kwak, B. R., Hermans, M. M., De Jonge, H. R., Lohmann, S. M., Jongsma, H. J., & Chanson, M. (1995). Differential regulation of distinct types of gap junction channels by similar phosphorylating conditions. *Mol Biol Cell, 6*(12), 1707-1719.

Kwak, B. R., & Jongsma, H. J. (1996). Regulation of cardiac gap junction channel permeability and conductance by several phosphorylating conditions. *Mol Cell Biochem, 157*(1-2), 93-99.

Kwak, B. R., Mulhaupt, F., Veillard, N., Gros, D. B., & Mach, F. (2002). Altered pattern of vascular connexin expression in atherosclerotic plaques. *Arterioscler Thromb Vasc Biol, 22*(2), 225-230.

Kyle, J. W., Berthoud, V. M., Kurutz, J., Minogue, P. J., Greenspan, M., Hanck, D. A., & Beyer, E. C. (2009). The N terminus of connexin37 contains an alpha-helix that is required for channel function. *J Biol Chem, 284*(30), 20418-20427. doi: 10.1074/jbc.M109.016907

Kyle, J. W., Minogue, P. J., Thomas, B. C., Domowicz, D. A., Berthoud, V. M., Hanck, D. A., & Beyer, E. C. (2008). An intact connexin N-terminus is required for function but not gap junction formation. *J Cell Sci, 121*(Pt 16), 2744-2750. doi: 10.1242/jcs.032482

Laemmli, U. K. (1970). Cleavage of structural proteins during the assembly of the head of bacteriophage T4. *Nature, 227*(5259), 680-685.

Lampe, P. D., & Lau, A. F. (2004). The effects of connexin phosphorylation on gap junctional communication. *Int J Biochem Cell Biol, 36*(7), 1171-1186. doi: 10.1016/s1357-2725(03)00264-4

Larson, D. M., Seul, K. H., Berthoud, V. M., Lau, A. F., Sagar, G. D., & Beyer, E. C. (2000). Functional expression and biochemical characterization of an epitope-tagged connexin37. *Mol Cell Biol Res Commun, 3*(2), 115-121. doi: 10.1006/mcbr.2000.0200

Liaudet, L., Vassalli, G., & Pacher, P. (2009). Role of peroxynitrite in the redox regulation of cell signal transduction pathways. *Front Biosci (Landmark Ed), 14*, 4809-4814.

Lima, B., Forrester, M. T., Hess, D. T., & Stamler, J. S. (2010). S-nitrosylation in cardiovascular signaling. *Circ Res, 106*(4), 633-646. doi: 10.1161/circresaha.109.207381

Looft-Wilson, R. C., Payne, G. W., & Segal, S. S. (2004). Connexin expression and conducted vasodilation along arteriolar endothelium in mouse skeletal muscle. *J Appl Physiol (1985), 97*(3), 1152-1158. doi: 10.1152/japplphysiol.00133.2004

Majesky, M. W., Dong, X. R., Hoglund, V., Mahoney, W. M., Jr., & Daum, G. (2011). The adventitia: a dynamic interface containing resident progenitor cells. *Arterioscler Thromb Vasc Biol, 31*(7), 1530-1539. doi: 10.1161/atvbaha.110.221549

Marquez-Rosado, L., Solan, J. L., Dunn, C. A., Norris, R. P., & Lampe, P. D. (2012). Connexin43 phosphorylation in brain, cardiac, endothelial and epithelial tissues. *Biochim Biophys Acta, 1818*(8), 1985-1992. doi: 10.1016/j.bbamem.2011.07.028

McKinnon, R. L., Bolon, M. L., Wang, H. X., Swarbreck, S., Kidder, G. M., Simon, A. M., & Tyml, K. (2009). Reduction of electrical coupling between microvascular endothelial cells by NO depends on connexin37. *Am J Physiol Heart Circ Physiol, 297*(1), H93-H101. doi: 10.1152/ajpheart.01148.2008

Megson, I. L., & Webb, D. J. (2002). Nitric oxide donor drugs: current status and future trends. *Expert Opin Investig Drugs, 11*(5), 587-601. doi: 10.1517/13543784.11.5.587

Miller, M. R., & Megson, I. L. (2007). Recent developments in nitric oxide donor drugs. *Br J Pharmacol, 151*(3), 305-321.

Morel, S., Burnier, L., & Kwak, B. R. (2009). Connexins participate in the initiation and progression of atherosclerosis. *Semin Immunopathol, 31*(1), 49-61. doi: 10.1007/s00281-009-0147-6

Morel, S., Burnier, L., Roatti, A., Chassot, A., Roth, I., Sutter, E., Kwak, B. R. (2010). Unexpected role for the human Cx37 C1019T polymorphism in tumour cell proliferation. *Carcinogenesis, 31*(11), 1922-1931. doi: 10.1093/carcin/bgq170

Munzel, T., Feil, R., Mulsch, A., Lohmann, S. M., Hofmann, F., & Walter, U. (2003). Physiology and pathophysiology of vascular signaling controlled by guanosine 3',5'-cyclic monophosphate-dependent protein kinase [corrected]. *Circulation, 108*(18), 2172-2183. doi: 10.1161/01.cir.0000094403.78467.c3

Murthy, K. S. (2006). Signaling for contraction and relaxation in smooth muscle of the gut. *Annu Rev Physiol, 68*, 345-374. doi: 10.1146/annurev.physiol.68.040504.094707

Pacher, P., Beckman, J. S., & Liaudet, L. (2007). Nitric oxide and peroxynitrite in health and disease. *Physiol Rev, 87*(1), 315-424. doi: 10.1152/physrev.00029.2006

Pezza, R. J., Villarreal, M. A., Montich, G. G., & Argaraña, C. E. (2002). Vanadate inhibits the ATPase activity and DNA binding capability of bacterial MutS. A structural model for the vanadate–MutS interaction at the Walker A motif. *Nucleic Acids Res, 30*(21), 4700-4708.

Pfenniger, A., Chanson, M., & Kwak, B. R. (2013). Connexins in atherosclerosis. *Biochim Biophys Acta, 1828*(1), 157-166. doi: 10.1016/j.bbamem.2012.05.011

Pfenniger, A., Derouette, J. P., Verma, V., Lin, X., Foglia, B., Coombs, W., Delmar, M. (2010). Gap junction protein Cx37 interacts with endothelial nitric oxide synthase in endothelial cells. *Arterioscler Thromb Vasc Biol, 30*(4), 827-834. doi: 10.1161/atvbaha.109.200816

Pogoda, K., Fuller, M., Pohl, U., & Kameritsch, P. (2014). NO, via its target Cx37, modulates calcium signal propagation selectively at myoendothelial gap junctions. *Cell Commun Signal, 12*(1), 33. doi: 10.1186/1478-811x-12-33

Rodenwaldt, B., Pohl, U., & de Wit, C. (2007). Endogenous and exogenous NO attenuates conduction of vasoconstrictions along arterioles in the microcirculation. *Am J Physiol Heart Circ Physiol, 292*(5), H2341-2348. doi: 10.1152/ajpheart.01061.2006

Rorig, B., & Sutor, B. (1996). Nitric oxide-stimulated increase in intracellular cGMP modulates gap junction coupling in rat neocortex. *Neuroreport, 7*(2), 569-572.

Rozen, S., & Skaletsky, H. (2000). Primer3 on the WWW for general users and for biologist programmers. *Methods Mol Biol, 132*, 365-386.

Rummery, N. M., & Hill, C. E. (2004). Vascular gap junctions and implications for hypertension. *Clin Exp Pharmacol Physiol, 31*(10), 659-667. doi: 10.1111/j.1440-1681.2004.04071.x

Sandow, S. L., Looft-Wilson, R., Doran, B., Grayson, T. H., Segal, S. S., & Hill, C. E. (2003). Expression of homocellular and heterocellular gap junctions in hamster arterioles and feed arteries. *Cardiovasc Res, 60*(3), 643-653.

Sandow, S. L., Neylon, C. B., Chen, M. X., & Garland, C. J. (2006). Spatial separation of endothelial small- and intermediate-conductance calcium-activated potassium channels (K(Ca)) and connexins: possible relationship to vasodilator function? *J Anat, 209*(5), 689-698. doi: 10.1111/j.1469-7580.2006.00647.x

Sandow, S. L., Senadheera, S., Bertrand, P. P., Murphy, T. V., & Tare, M. (2012). Myoendothelial contacts, gap junctions, and microdomains: anatomical links to function? *Microcirculation, 19*(5), 403-415. doi: 10.1111/j.1549-8719.2011.00146.x

Schmidt, V. J., Wolfle, S. E., Boettcher, M., & de Wit, C. (2008). Gap junctions synchronize vascular tone within the microcirculation. *Pharmacol Rep, 60*(1), 68-74.

Shevchenko, A., Tomas, H., Havlis, J., Olsen, J. V., & Mann, M. (2006). In-gel digestion for mass spectrometric characterization of proteins and proteomes. *Nat Protoc, 1*(6), 2856-2860. doi: 10.1038/nprot.2006.468

Simon, A. M., & McWhorter, A. R. (2003). Decreased intercellular dye-transfer and downregulation of non-ablated connexins in aortic endothelium deficient in connexin37 or connexin40. *J Cell Sci, 116*(Pt 11), 2223-2236. doi: 10.1242/jcs.00429

Sohl, G., & Willecke, K. (2003). An update on connexin genes and their nomenclature in mouse and man. *Cell Commun Adhes, 10*(4-6), 173-180.

Sohl, G., & Willecke, K. (2004). Gap junctions and the connexin protein family. *Cardiovasc Res, 62*(2), 228-232. doi: 10.1016/j.cardiores.2003.11.013

Solan, J. L., & Lampe, P. D. (2009a). Connexin43 phosphorylation: structural changes and biological effects. *Biochem J, 419*(2), 261-272. doi: 10.1042/bj20082319

Solan, J. L., & Lampe, P. D. (2009b). CONNEXIN 43 PHOSPHORYLATION – STRUCTURAL CHANGES AND BIOLOGICAL EFFECTS. *Biochem J, 419*(2), 261-272.

Stergiopoulos, K., Alvarado, J. L., Mastroianni, M., Ek-Vitorin, J. F., Taffet, S. M., & Delmar, M. (1999). Hetero-domain interactions as a mechanism for the regulation of connexin channels. *Circ Res, 84*(10), 1144-1155.

Straub, A. C., Billaud, M., Johnstone, S. R., Best, A. K., Yemen, S., Dwyer, S. T., Isakson, B. E. (2011). Compartmentalized connexin 43 s-nitrosylation/denitrosylation regulates heterocellular communication in the vessel wall. *Arterioscler Thromb Vasc Biol, 31*(2), 399-407. doi: 10.1161/atvbaha.110.215939

Straub, A. C., Zeigler, A. C., & Isakson, B. E. (2014). The myoendothelial junction: connections that deliver the message. *Physiology (Bethesda), 29*(4), 242-249. doi: 10.1152/physiol.00042.2013

Thomas, M. A., Huang, S., Cokoja, A., Riccio, O., Staub, O., Suter, S., & Chanson, M. (2002). Interaction of connexins with protein partners in the control of channel turnover and gating. *Biol Cell, 94*(7-8), 445-456.

Tousoulis, D., Kampoli, A. M., Tentolouris, C., Papageorgiou, N., & Stefanadis, C. (2012). The role of nitric oxide on endothelial function. *Curr Vasc Pharmacol, 10*(1), 4-18.

Traub, O., Hertlein, B., Kasper, M., Eckert, R., Krisciukaitis, A., Hulser, D., & Willecke, K. (1998). Characterization of the gap junction protein connexin37 in murine endothelium, respiratory epithelium, and after transfection in human HeLa cells. *Eur J Cell Biol, 77*(4), 313-322. doi: 10.1016/s0171-9335(98)80090-3

Veenstra, R. D., Wang, H. Z., Beyer, E. C., Ramanan, S. V., & Brink, P. R. (1994). Connexin37 forms high conductance gap junction channels with subconductance state activity and selective dye and ionic permeabilities. *Biophys J, 66*(6), 1915-1928. doi: 10.1016/s0006-3495(94)80985-3

Wagner, C. (2008). Function of connexins in the renal circulation. *Kidney Int, 73*(5), 547-555. doi: 10.1038/sj.ki.5002720

Weber, P. A., Chang, H. C., Spaeth, K. E., Nitsche, J. M., & Nicholson, B. J. (2004). The permeability of gap junction channels to probes of different size is dependent on connexin composition and permeant-pore affinities. *Biophys J, 87*(2), 958-973. doi: 10.1529/biophysj.103.036350

Widmaier E. P., R. H., Strang K. T., and Vander A. J. . (2008). *Vander's human physiology: The mechanisms of body function* (Vol.).

Yamamoto, T., & Bing, R. J. (2000). Nitric oxide donors. *Proc Soc Exp Biol Med, 225*(3), 200-206.

ABBREVIATION

A	Alanine
Å	Angstrom
aa	Amino acid
Ab / Abs	Antibody / Antibodies
ANOVA	one-way analysis of variance for repeated measures
ATP	Adenosine triphosphate
bp	Base pair
BSA	Bovine serum albumin
C	Celsius oder Culture
Ca^{2+}	Calcium ions
CaMKII	$Ca^{2+/}$CaM-dependent kinase II
cAMP	Cyclic Adenosinmonophosphate
cAMP-PKA	cAMP-dependent protein kinase
cDNA	Complementary deoxyribonucleic acid
cGMP	3`-5`cyclic guanosine monophosphate
cl	Cytoplasmic loop
CO_2	Carbon dioxide
COOH, C-terminus	Carboxyl terminus
c-Src	Proto-oncogene tyrosine-protein kinase Src
Cx (Cxs)	Connexin (Connexins)
Cx37 or GJA4	Connexin 37
Cx37GFP	Connexin 37 full length protein (aa 1 – 333), GFP tagged
Da	Daltons
DMEM	Dulbecco's Modified Eagle Medium
DMSO	Dimethylsulfoxide
DNA	Deoxyribonucleic acid
DNTP	Deoxyribonucleotide triphosphates

ABBREVIATION

DTT	Dithiothreitol
EC	Endothelial cells
EDHF	Endothelium-derived hyperpolarizing factor
EDTA	Ethylenediaminetetraacetic acid
el1, el2	Extracellular loop
eNOS	Endothelial NOS-3 synthase
eNOS	Endothelial NO synthase
FCS	Fetal calf serum
for	Forward
For_1Cx37	Primer forward Cx37
Fura 2AM	Fura 2AM -acetoxymethyl
g	$g=9.8m/s^2$
GFP	Green fluorescent protein
gfp-for	Primer forward GFP
Gfp-rev	Primer reverse GFP
GJ	Gap junction
GJC	Gap junctions communication
GJs	Gap junctions
GSK-3	Glycogen synthase kinase-3
H_2O	water
H_2O_2	Hydrogen peroxide
HeLa	Henrietta Lacks (Immortal cervix carcinoma cells)
HEPES	4-(2-hydroxyethyl)-1-piperazineethanesulfonic acid
HPLC	High Performance Liquid Chromatography
IHC	Immunohistochemsitry
IPI	International Protein Index (human database)
kDa	Kilo daltons
KO	Knockout
l	Liter
LC-MS/MS	Tandem mass spectrometry
LNA	N-nitro-L-arginine

ABBREVIATION

m	Mili
m1,m2,m3,m4	Transmembrane domains
MAPK	Mitogen-activated protein kinase
MEGJ	Myoendothelial gap junctions
MEGJs	myoendothelial gap junctions
min	Minute
ml	Milliliter (10^{-3} liter)
mRNA	Messenger ribonucleic acid
N	Nucleus
n	Number of experiments
NCBS	New born calf serum
NH_2 / N-terminus	Amino-terminus
nm	Nano meter
NO	Nitric oxide
NOS	NO synthase
ODQ	guanylyl cyclase inhibitor - oxadiazole-[4,3-a]-quinoxalin-1-one
ONOO-	Peroxynitrite
P/ Pro	Proline
PBS-	Mg^{2+}-Ca^{2+} free phosphate buffered saline
PBS+	Phosphate buffered saline
pO_2	Pressure of oxygen
pCO_2	pressure of carbon dioxide
PCR	Polymerase chain reaction
PKA	Protein kinase A
PKC	Protein kinase C
PKG	Protein kinase G
PKG	Protein kinase G
PLC	phospholipase C
pmol	Picomoli
PMSF	Phenylmethylsulfonyl fluoride
pS	Picosiemens (dimesion unit of the electrical conductance)

PTM	Posttranslational modification
rev	Reverse
Rev_1Cx37	Primer reverse Cx37
RLT	Buffer denaturing guanidine-thiocyanate containing buffer with 10 µl/ml ß-mercaptoethanol
RNA	Ribonucleic acid
RNase	Ribonuclease
ROI	Regions of interest
RP	Reversed phase
rpm	Rounds per minute
RT	Room temperature
RT-PCR	Reverse Transcription-Polymerase Chain Reaction
s	Second
SDS	Sodium dodecylsulfate
SDS-PAGE	SDS-Polyacrylamid gel electrophoresis
SEM	Standard error of the mean
Ser	Serine
SMC	Smooth muscle cells
SNAP	S-nitroso-N-acetyl-D,L- penicillamine
SNP	sodium nitroprusside
SOD	Superoxide dismutase
TBE	Tris-borate-EDTA
TBS	Tris buffered saline
TBS-Tween / TBS-T	Tris buffer saline Tween
TFA	Trifluoroacetic acid
Thr	Threonine
TiO_2	Titanium dioxide
Tyr/ Y	Tyrosine
V	Volts
VSM	Vascular smooth muscle
VSMC	Vascular smooth muscle cells

ABBREVIATION

w	Wells
WB	Western blot
wt	Wild-type

VI. ACKNOWLEDGEMENTS

The work of this thesis was performed in the laboratories of the Walter-Brendel-Centre of Experimental Medicine in Munich. During the years I spent working on Connexins, I learned so much and this thesis would not have been possible if it wasn´t for a number of important people. At this point, I would like to take the opportunity and say ``thank you``:

I would like to express my thanks to Prof. Dr. Ulrich Pohl for giving me the opportunity doing the present doctoral thesis at Walter-Brendel-Centre of Experimental Medicine in Munich and for his great scientific support during this time, fruitful discussions and helpful suggestions.

I have been lucky to participate in Small Artery Remodeling Network. For this opportunity I am immensely grateful and would like to acknowledge all members of the network.

My supervisor Dr. Petra Kameritsch for overall support in many ways, introduction to connexion project, limit-less time for interesting discussions but also relaxed chats, numerous suggestions and support during the final phase of my work.

Thanks to Silvia Münzing for helping me in the lab and technical assistance and for printing posters and Dr Krisitin Pogoda for the HeLa Cx37GFP and mutants cells used in the thesis.

Moreover, I would like to thank my colleagues Dr. Julian Kirsch, Dr. Theres Hennig and Stefan Schmitt, Matthias Semisch for their help during my experiments and also for all talks during lunch, coffee break or after work.

Thanks to all technicians of the Pohl group for technical support and help at any time in the lab.

I would like to thank you for proof-reading the manuscript to: Dr. Eva Almajan, Dr. Mihaela Bacalum, Msc. Adina Mihai, Andrei Galbenu, Dr. Oana Bodea and Liviu Bodea, Cristina Saftoiu.

Thank you mother for your unquestioning support during this time and also for your love!

Finally, Thanks to my friends for also being just a phone call away, listening and for believing in me, standing behind me and having the time and patience when nobody would. Thank you for your optimism and also constant positive thinking. With you by my side I had the feeling that I can do it.

VII. CV

Laurenția-Irina Tănase

Personal Information

Date of Birth	24 September 1983
Place	Calarasi, Romania

Education

09/2010 – 2014	**PhD Study** - Ludwig-Maximilians-Universität, Walter-Brendel-Zentrum, Munich- Germany
09/2007 – 07/2009	**Master of Science – Neurobiology** Faculty of Biology, University of Bucharest, Romania
09/2003 – 07/2007	**Bachelor of Science – Biochemistry** Faculty of Biology, University of Bucharest, Romania

Work Experience

09/2010 – 08/2013	**PhD Student in the research training programme Marie Curie of the European Commission „Small Artery Remodelling" (SmArt)** *Ludwig-Maximilians-Universität, Walter-Brendel-Zentrum, Munich, Germany*
02/2008 – 08/2010	**Research Assistant** *Institute of Cell Biology and Pathology "Nicolae Simionescu", Bucharest-Romania, Vascular Cell Biology and Molecular Genetics Department*

Publications

Manea A, Tanase L., Raicu M., Simionescu M., ***Transcriptional regulation of NADPH oxidase isoforms, Nox1 and Nox4, by nuclear factor-kB in human aortic smooth muscle cells*.** Biochem Biophys Res Commun. 2010 May.

Manea A, Tanase L., Raicu M., Simionescu M., ***JAK/STAT3 signaling pathway regulates Nox1 and Nox4-based NADPH oxidase in human aortic smooth muscle cells*.** Arteriosclerosis, Thrombosis, and Vascular Biol., 2010 Jan; 30(1):105-12.

Raicu M., Tanase L., Manea A., ***Different effect of felodipine and amlodipine on NADPH oxidase expression and function in human smooth muscle cells*.** Annals of RSCB, vol. XIV, pag 9, 2009 Dec.

Trainings

2013	1.PhD-course Careers in Biomedicine, Lund, Sweden, 13-14 June **(poster)**
2012	1. European SmArt Workshop on Proteomics and Vascular Biology London, United Kingdom 27-29 March

2011 1. Mechanotransduction and Modelling of the Vascular Wall Workshop, Rebild, Denmark, 8-12 May

2. Bioimaging Workshop and Midterm Evaluation Meeting, Munich, Germany 13–16 October

2010 1. First SmArt Workshop on Extracellular Matrix of the Vessel Wall, Munster, Germany, 2-5 October

2008 1. The promise of Stem Cells Therapy Workshop, Bucharest, Romania, 11-12 April

2. From Gene Expression and Protein Activation to Human Diseases Workshop, Bran, Romania, 16-20 April

3. Pathologies, Pharmacology and Molecular Biotechnology, XIV-th French Summer School, Arad, 7-19 July

4. From Basic Research Discoveries to Therapeutic Applications Workshop Biomedicine, Bucharest, 17-18 September

5. From Cellular and Molecular Biology to the XXIst Century Medicine, VIII-th Postgraduate course, Bucharest, 20-29 October

Congresses

1. Symposium on Vascular Signalling mechanisms, Lund, Sweden, June 2013 **(poster)**
2. Frontiers in Cardiovascular Biology London, United Kingdom, March- April 2012 **(poster)**
3. Vascular Progenitors in Biology and Medicine, Fribourg, Switzerland, September 2012 **(poster)**
4. 10th International Symposium on Resistance Arteries, Rebild, Denmark, May 2011 **(poster)**
5. Marie Curie Symposium „SCIENCE –Passion, Mission, Responsibilities", Warsaw, Poland, September 2011 **(poster)**
6. Joint Meeting of the ESM and GfMVB Munich, Germany October 2011 **(poster)**

Oral presentations

8.12.2011- 10.12.2012	Munich – Pecs (presentation)
15.01.2012 – 17.01.2012	Pécs visit in Munich, (presentation)
3 December 2012	Seminar WBex (presentation)
12 March 2013	WBex Phd student day (presentation)

Eidesstattliche Versicherung

Tanase Laurentia Irina

Name, Vorname

Ich erkläre hiermit an Eides statt,

dass ich die vorliegende Dissertation mit dem Thema

The C-terminus of Cx37 as target of nitric oxide dependent modification of gap junction permeability

selbständig verfasst, mich außer der angegebenen keiner weiteren Hilfsmittel bedient und alle Erkenntnisse, die aus dem Schrifttum ganz oder annähernd übernommen sind, als solche kenntlich gemacht und nach ihrer Herkunft unter Bezeichnung der Fundstelle einzeln nachgewiesen habe.

Ich erkläre des Weiteren, dass die hier vorgelegte Dissertation nicht in gleicher oder in ähnlicher Form bei einer anderen Stelle zur Erlangung eines akademischen Grades eingereicht wurde.

München, 7.03.2016

Ort, Datum

Unterschrift Doktorandin/Doktorand